EXPERIMENTAL INVESTIGATION OF THE PRESSURE DISTRIBUTION IN A REGENERATIVE TURBINE PUMP, THE STA-RITE TH-7

by

Gilbert F. Lutz

Submitted in partial fulfillment of the requirements
for the degree of Bachelor of Science
at the
MASSACHUSETTS INSTITUTE OF TECHNOLOGY
May 25, 1953

Signature of author Signature redacted
Dept. of Mechanical Engineering

Certified by Signature redacted
Thesis Advisor

May 25, 1953

Professor Earl B. Millard
Secretary of the Faculty
Massachusetts Institute of Technology
Cambridge, Massachusetts

Dear Sir:

In partial fulfillment of the requirements for the degree of Bachelor of Science in Mechanical Engineering from the Massachusetts Institute of Technology, I submit this thesis entitled "Experimental Investigation of the Pressure Distribution in a Regenerative Turbine Pump, the Sta-Rite TH-7".

Respectfully,

Signature redacted

Gilbert F. Lutz

ACKNOWLEDGEMENT

The author wishes to express his appreciation to Professors Wadleigh and Wilson for their advice and personal interest. Special thanks are due John Oelrich and Miguel Santalo for their assistance in planning and conducting the experiments. To Vern Steeves and the personnel of the Mechanical Engineering Shop, thanks for your help in modifying and preparing the pump for investigation.

ABSTRACT

The pressure distribution within a regenerative turbine pump, the Sta-Rite TH-7, was investigated. Graphs of performance, pressure versus angle, pressure versus radius, and the rate of change of pressure with angle versus through-flow were plotted. Conclusions concerning the general performance of the pump, the behavior of the fluid flow within the pump, and the characteristics of the important parameters were drawn from the graphs.

Table of Contents

Introduction

Experimental investigation of the Sta-Rite TH-7, a regenerative turbine pump, was begun in the fall of 1952 by a group of four seniors working in two pairs. The first pair, Daniel A. Lippman and Theodore Taylor, Jr., designed and constructed the test equioment and made certain modifications in the pump. The second pair, Thomas J. Hopkins and Luis R.Lazo, attempted a general theoretical and experimental analysis of the pump, working in conjunction with John A. Oelrich, an engineer from the Research and Development Department of the Worthington Corporation.

In the course of the theoretical analysis, it was necessary to make ceratain fundamental assumptions. Because of the time consumed in the construction of the test apparatus and the development of the theory, they were unable to verify all the assumptions before the end of the term. For this reason, and because experimental data was required to check further developments in the theory, it was decided to continue the investigation of the pressure distribution and the flow characteristics within the pump.

One of the major assumptions made was that the flow patterns within the pump were essentially the same from entrance to exit. In other words, a picture of these patterns taken anywhere within the pump (suitably removed from exit and/or inlet conditions) would accurately

describe the system. In order to check this assumption and also to obtain data for use in the theory, measurements were made of pressure as a function of both radius (r) and angle (θ).

The rate of change of pressure with respect to angle, $dp/d\theta$, was determined graphically to ascertain whether it was unaffected by angular position, i.e., a constant.

A general picture of $dp/d\theta$ with respect to radius and through-flow (Q) was sought. An investigation of the rate of change of pressure with respect to radius, (dp/dr), was undertaken with the hope that it would yield information as to the general action of the pump, in particular, whether rigid body rotation was approached near the point of zero head rise.

It was felt that a better approximation of the point of maximum efficiency might be obtained if higher flows through the pump were induced by means of a vacuum at the outlet, and so this possibility was also examined.

Finally, in an effort to confine the streamline pattern to a relative simple and constant shape, a shroud was installed upon a standard rotor, and the assembly was put through the above tests. It was hoped that this modification would disclose significant trends in head and efficiency, and that it would induce a flow similar to the assumed one.

Throughout the program, an effort was made to secure quantitative results for use in the theoretical development being conducted by John Oelrich and Miguel Santalo.

Pump Modifications

In order to measure the different pressures with respect to both angle and radius, it was necessary to install an extensive series of pressure taps. Eleven taps were installed in the front head, and six more in the case. Since previous experimenters had already placed four taps in the case, the additional ones made a total of ten. Blueprints of drawings#1 and #2 clearly show the dimensions and the locations of the holes made to receive them.-

The taps in the case proved to be the easiest to install. Thin-walled, seamless, stainless steel tubing with an outside diameter of .120" was used in order to obtain the largest inside diameter possible with a given outside diameter. A large inside diameter was desirable in order to reduce the response time-lag of the manometers. At the same time, the outside diameter of the tubing was strictly limited by the distance between paired taps.

The taps in the head at radii of 2.1" and 2.4" were not difficult to install. Because of the entrance passage in the interior of the casting, it was necessary to drill through only about a half inch of cast iron. The fact that that last quarter inch of this was some distance removed from the first caused difficulty only with the last hole (clockwise) made at the 2.4" radius. Here the fillet of the

---

*See Descriptive Appendix

thickening passage wall threatened to bend and break the small (#53) drill. Accordingly , the drill was withdrawn and another hole made from the outside. Although every effort was made to align the two, there proved to be a difference of about 1/16th of an inch between the opening of the second hole and the point struck by the tubing inserted through the first. Because the point in question could be seen and reached from the fluid entrance and because the tubing was thin and fairly flexible, it was possible to bend it enough (without giving it a permanent set) to enable it to pass through the second hole. The presence of this encroaching fillet practically limits the number of taps at this radius to the present number (3).

Since it was necessary to pass the taps through the inlet passage, stainless tubing was used to minimize the obstruction to the flow. Furthermore , the taps at different radii were spaced at least one bucket width (9 degrees) apart to help reduce the throttling effect. Here the size of the tubing should be as small as possible and is effectively established by the response-lag you are willing to put up with. Accordingly, the tubing used at radii of 2.1" and 2.4" had an outside diameter of 4o thousandths of an inch, and its outside measured 58 thousandths.

A larger tube was used for the taps located at a radius of 1.812" to make it easier to hit when drilling in from the side. After the tube was in place and the side hole drilled, a wire was inserted through the smaller side hole, and the inside end of the larger passage was

tapped to receive a small screw with solder coated threads. The assembly was then heated to set the solder, the wire withdrawn, and the excess screw cut off. A few passes with a grinder removed the rough part remaining.

To prevent these taps from being affected by leaks from the entry passage, they were sealed with cement applied through the entrance. The installation of more taps at this radius is clearly limited to that area which can be reached with sealing cement from the entrance.

In summary, it does not seem feasible to make taps cover a larger arc at radii of 1.812" and 2.4", than that presently covered. No such limitation exists for the ones at a radius of 2.1". Finally, if leaks occur within the head assembly, they are most likely to be found at the inner points sealed with cement.

Pictorial views of the head are in Plates 2 and 3 in the Descriptive Appendix.

Testing Procedure

As in the previous experiments, it was decided to use air as the working fluid. The pressure taps were connected by means of rubber and plastic flexible tubing to water manometers. The original equipment included a small manometer board mounting eight tubes, but the large number of taps made this inadequate. An additional board mounting sixteen tubes was secured, and the combination proved satisfactory for the purposes of the investigation. An Electro-Lux vacuum cleaner was employed to create a partial vacuum at the outlet and thus enable the pump to operate at higher through-flows than would otherwise be attainable.*

In an effort to obtain a more stable voltage source, a direct current motor-generator set was tried. Unfortunately, the voltage output proved even less stable than that obtainable from the ordinary alternating current outlet, and it was regretfully abandoned.

Speed control was finally achieved with a variable transformer. However, with this device voltage fluctuations in the line were passed on to the apparatus and caused marked changes in speed. Absence of a voltage regulating device made it necessary to employ a man constantly at the transformer to compensate for line voltage variations. Actually, two men are necessary to operate the apparatus and record data during an experiment, but three are desirable because of the large number of obser-

* See Plate 1, Descriptive Appendix

vations which must be made.

Speed variations were measured with a Strobetac. To make sure that a harmonic was not being recorded, a tachometer with a large diameter pickup wheel was used to check the readings. Since it was desired that the speed be held constant, the Strobotac was always set on line when the experiment was being conducted. Thus an accidental brush against the control wheel would not disturb the setting. As a result, all the data was obtained while the pump was operating at a speed of 3600 revolutions per minute.

During a test run, an Electro-Lux vacuum cleaner was employed as a blower to cool the dynamometer motor. When torque readings were being taken, the blower was shut off lest the air stream should induce an error.

During the run, one man stayed at speed control and made small adjustments in the variable transformer to hold a constant speed. If the speed tended to wander appreciably, he would call out to the man taking observations and that man would stop work until the speed was once again constant at 3600 revolutions per minute. At the end of each run, the temperature and pressure of the atmosphere were recorded. Before making the run for torque measurement, the dynamometer was disassembled and cleaned and lubricated as directed in the design thesis.*

---

*D.Lippman and T.Taylor, "Design and Construction of Test Equipment for a Regenerative Fluid Pump"

Accuracy

Great pains were taken to locate accurately the positions of the pressure taps. Much of the work of location was done by a professional shop man using an inscribing tool mounted on a small stand. When used in conjunction with a ground flat surface, such a tool can measure and inscribe lines with great accuracy. This task was facilitated since both the head and the case had surfaces machined to close tolerances which could be set against the large flat one. It is conservatively estimated that these holes were located within .020" of the points desired.

The holes in the front head were drilled from the inside or measuring surface out, and consequently the tendency of the drill to drift can be neglected for them. The holes in the case had to be drilled from the outside, but since the depth of drilling was only about ¼", the drift of the drill is probably negligible here.

When the small tubes were installed in the head, they were allowed to project about ½" above the inside surface. This was done to prevent them from filling with solder when they were soldered to the inside surface. After the soldering was completed, they were cut off as close to the head as possible and excess solder and tube filed off. After the job was finished with emery paper, no roughness could be felt with the finger in the area. The tube was

still solidly secured by the ring of solder which filled the counterbored cavity. In some cases it was not possible to fill completely these cavities. In these places a very small touch of modelling clay was used to make the approach to the tap perfectly flat. Because of the care taken to eliminate surface imperfections near the tap, it is felt that errors from this source may be neglected.*

Water was used in vertical manometers to measure pressures. The manometer stand was carefully levelled before the experiments were begun so that the same zero reading was obtained for all of them. A grid behind the manometers was marked in tenths of an inch. It was possible to read the pressures in all tubes , except that one which was open to the atmosphere, to within .025". The atmospheric tube could be read to this accuracy at shut-off, but as the flow control valve was opened, the small speed fluctuations of the dynamometer caused slight changes in the levels of the other fifteen tubes. Since all sixteen were interconnected, the cumulative fluctuation made itself felt in the two places which were at constant (atmospheric) pressure, the reservoir and the atmospheric tube. The result gave rather large fluctuations in the level of the latter. It is estimated that under the worst conditions, the level of this tube could be read to the nearest tenth of an inch.

---

*The solder rings and clay surfacing may be seen in Plate 3 of the Descriptive Appendix.

Barametric pressure and temperature were taken before each run. Since the data was graphed separately and since the differences were very slight for these two quantities, no attempt was made to adjust the results to the same base. These figures are given in the Calculations Appendix in the event that future investigations should make such a correction desirable.

In summary, it is believed that pressure measurements recorded are quantitatively accurate to within .2".

Results and Conclusions

Standard Impeller

By using a vacuum at the outlet, it was possible to extend the dimensionless plot of head versus through-flow rate to the point of zero head rise across the pump. This point falls at a through-flow rate, $\frac{Q}{\omega D^3}$, of 9×10^{-3}. If we substitute 120π for w, and the diameter of the impeller, 5.393", for D, we obtain an actual through-flow of .308 cubic feet per second for the through-flow at a condition of zero head rise. Needless to say, this is also the condition for zero efficiency.

An examination of Fig.1, the plot of head versus through-flow rate, yields the information that the head rise is a linear function of the through-flow between the values for $\frac{Q}{\omega D^3}$ of 2.5×10^{-3} and 6.5×10^{-3}. The equation for this line is given below:

$$\frac{gH}{\omega^2 D^2} = 1.1 - 212.5 \frac{Q}{\omega D^3}$$

If the pump exhausts to atmospheric pressure, the above expression will hold true up to the highest attainable flow-rate.

No such simple relationship exists for either of the dimensionless plots of power versus flow-rate, Fig.'s 2 and 3. The brake power required at zero head rise was not graphed. The value of $\frac{gH}{\omega^2 D^2}$ at this point was .00194.

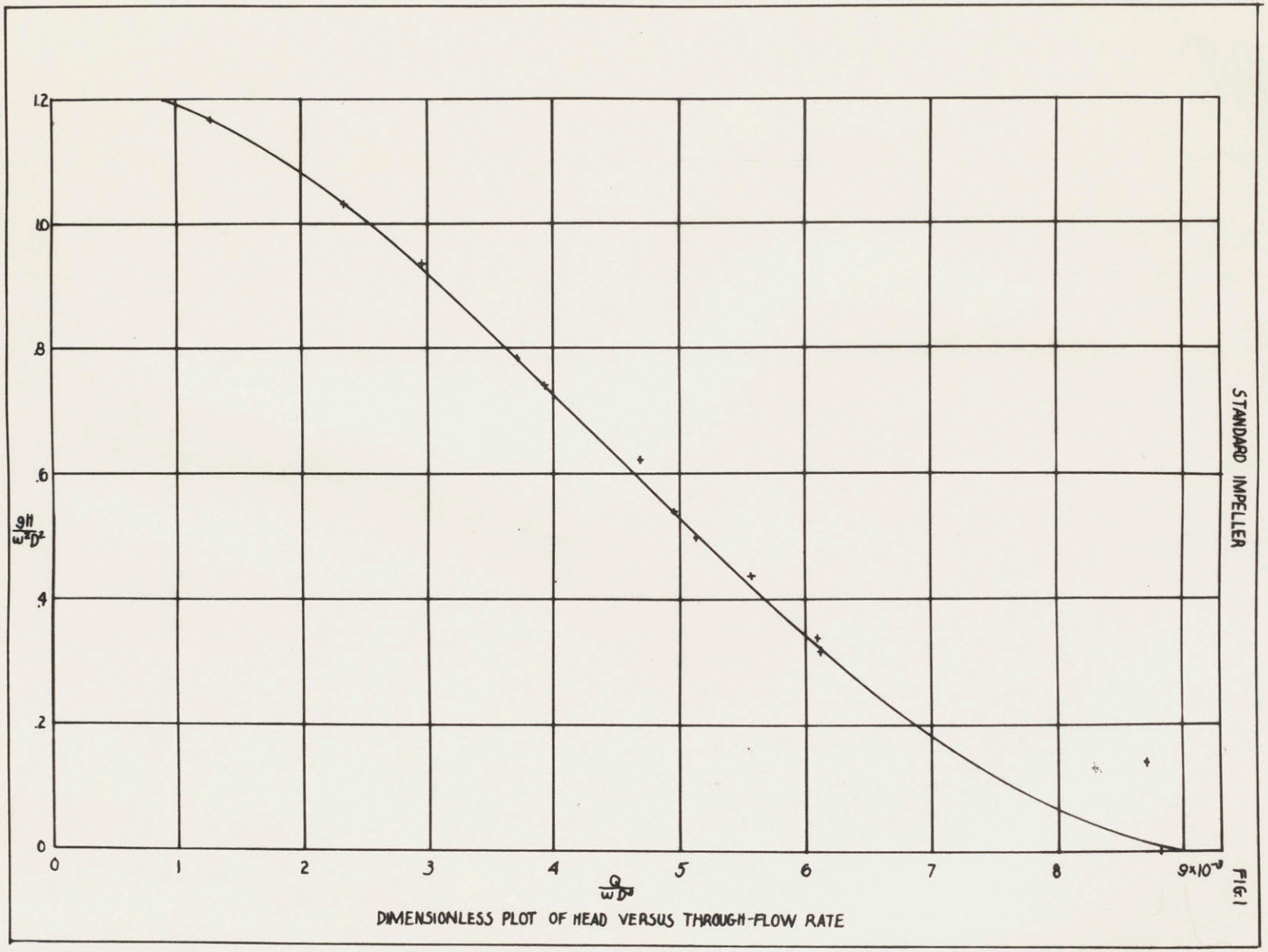

DIMENSIONLESS PLOT OF HEAD VERSUS THROUGH-FLOW RATE

FIG. 2

STANDARD IMPELLER

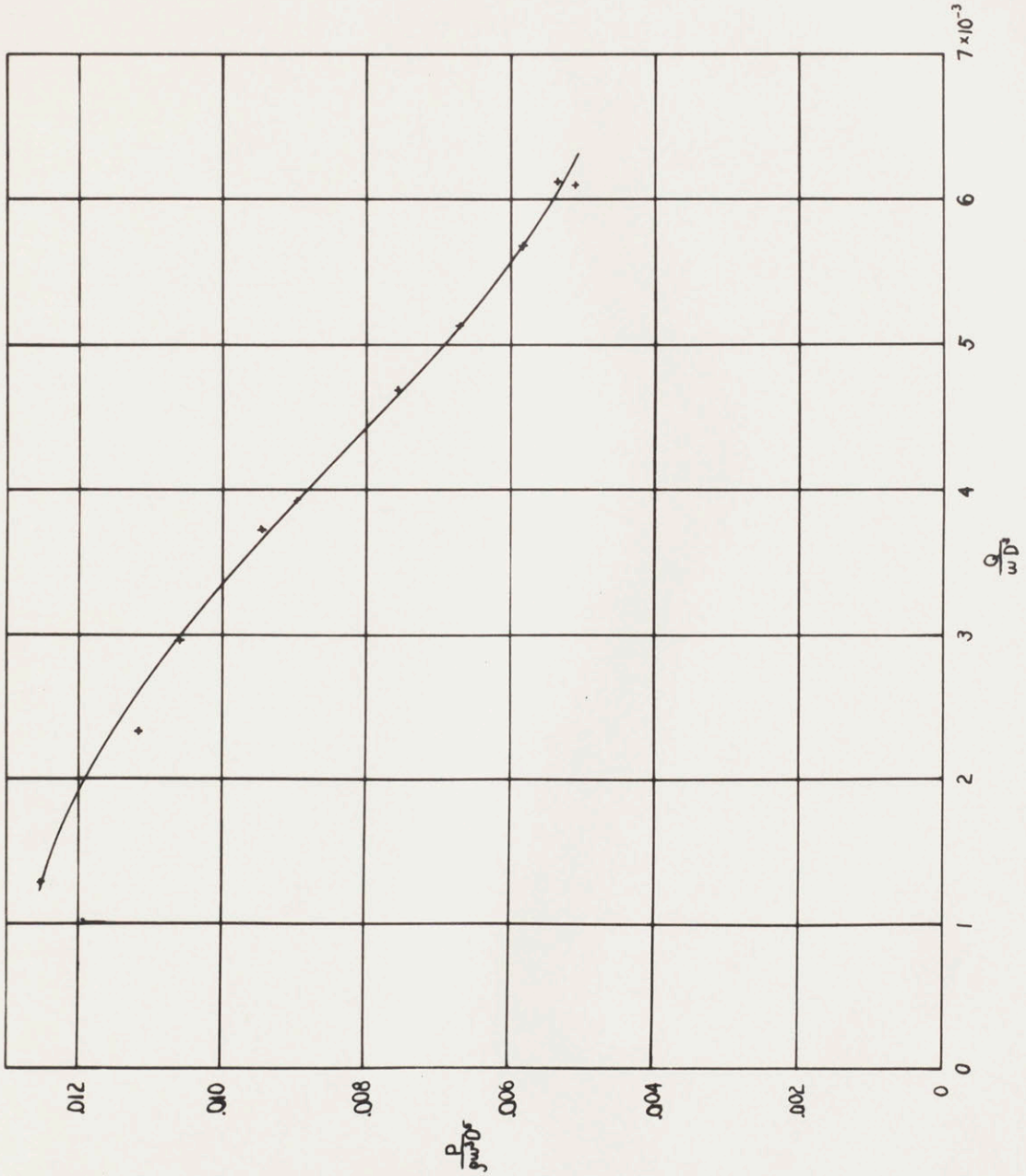

DIMENSIONLESS PLOT OF POWER(BRAKE) VS. FLOW RATE

From Figure 3 we can see that maximum useful power* is transmitted to the fluid at a $\frac{Q}{wD^3}$ of about 4.7×10^{-3}.

A maximum value for the efficiency was found to be 42.5%. The points determined using the vacuum at the outlet were not necessary for the definition; however, they are plotted in Fig.4A and cause no marked change in the curve of Fig.4.

The maximum value obtained for the efficiency is less than that obtained by the builders of the apparatus. A check with an independent laboratory group** which had the opportunity to test the apparatus yielded a similar curve, with an even lower maximum. The curve derived by this group also showed a clearly defined maximum at a value of $\frac{Q}{wD^3}$ very close to the 5.7×10^{-3} noted on Fig.4. It is suggested that the slightly higher maximum (45%) obtained by the builders could be attributed to their greater familiarity with the cleaning and adjustment of the apparatus. From the nature of Fig. 4, it is apparent that there is little point in operating the present pump beyond a $\frac{Q}{wD^3}$ of 6.4×10^{-3}.

---

* See Calculations Appendix for definition of useful horsepower.

**2.68 Laboratory Exercise B-2, Group I, F. J. Ryan-Group Leader

FIG. 3

STANDARD IMPELLER

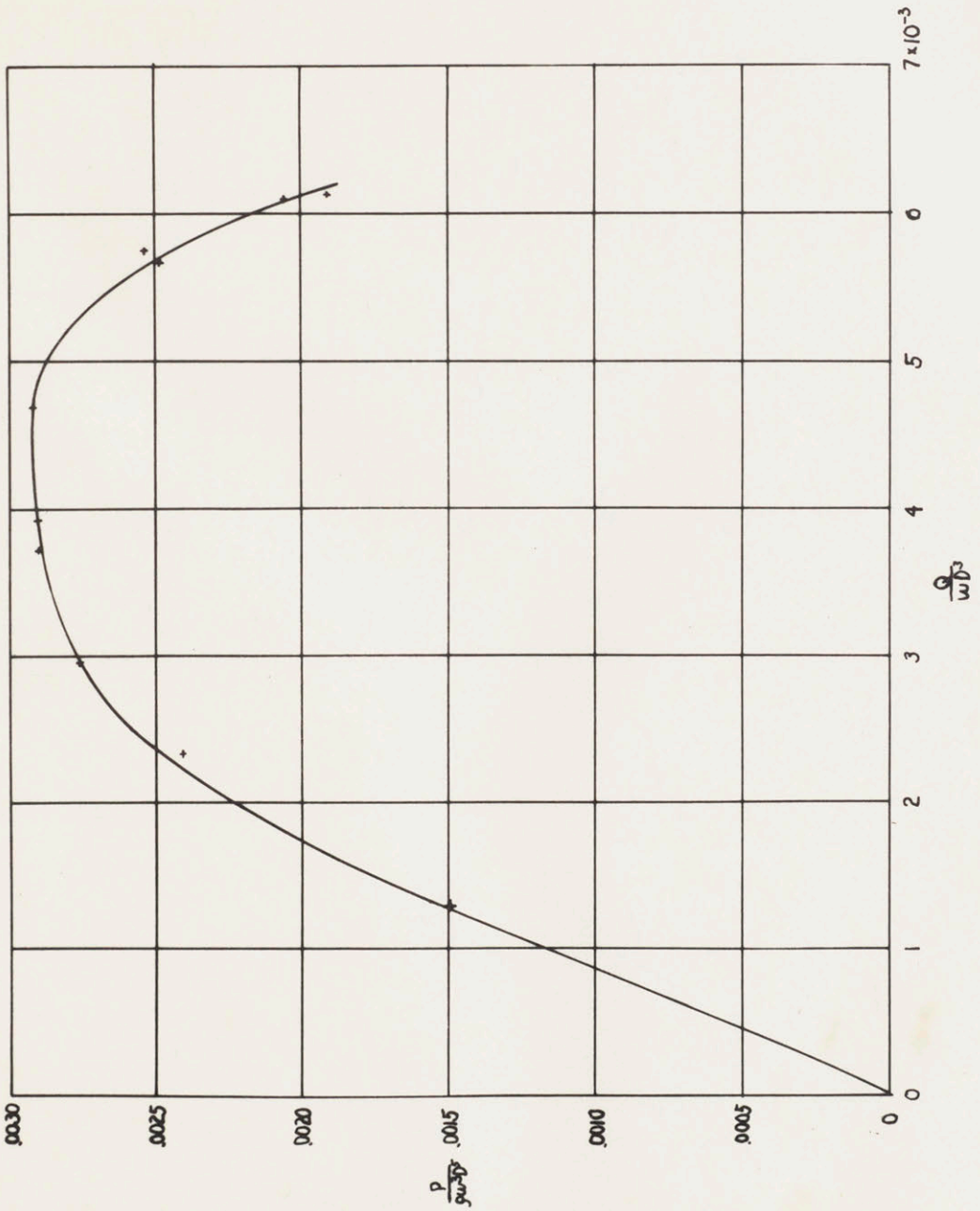

DIMENSIONLESS PLOT OF POWER(USEFUL) VERSUS THROUGH-FLOW RATE

FIG. 4

STANDARD IMPELLER

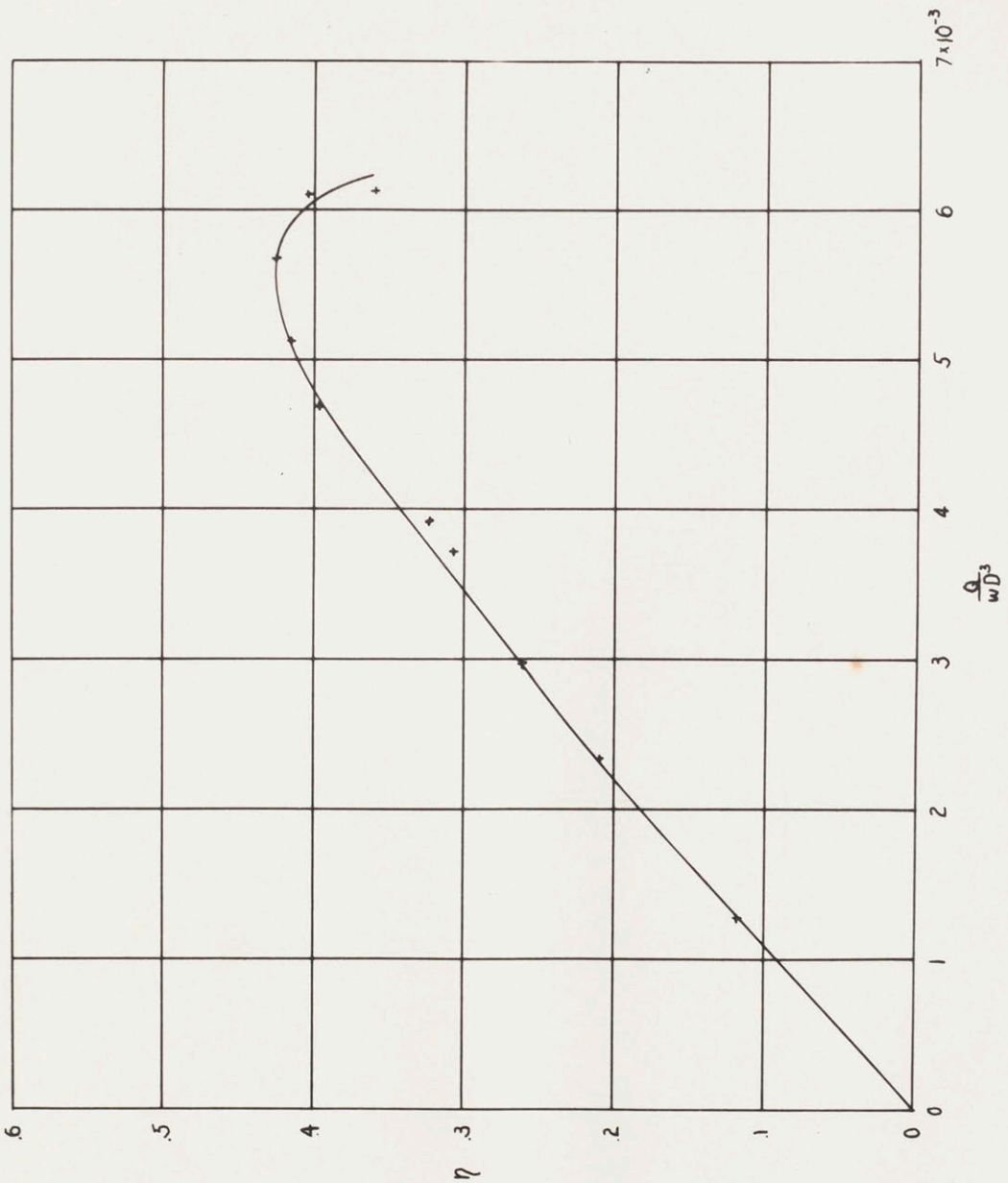

DIMENSIONLESS PLOT OF EFFICIENCY VERSUS THROUGH-FLOW RATE

FIG. 4A

STANDARD IMPELLER

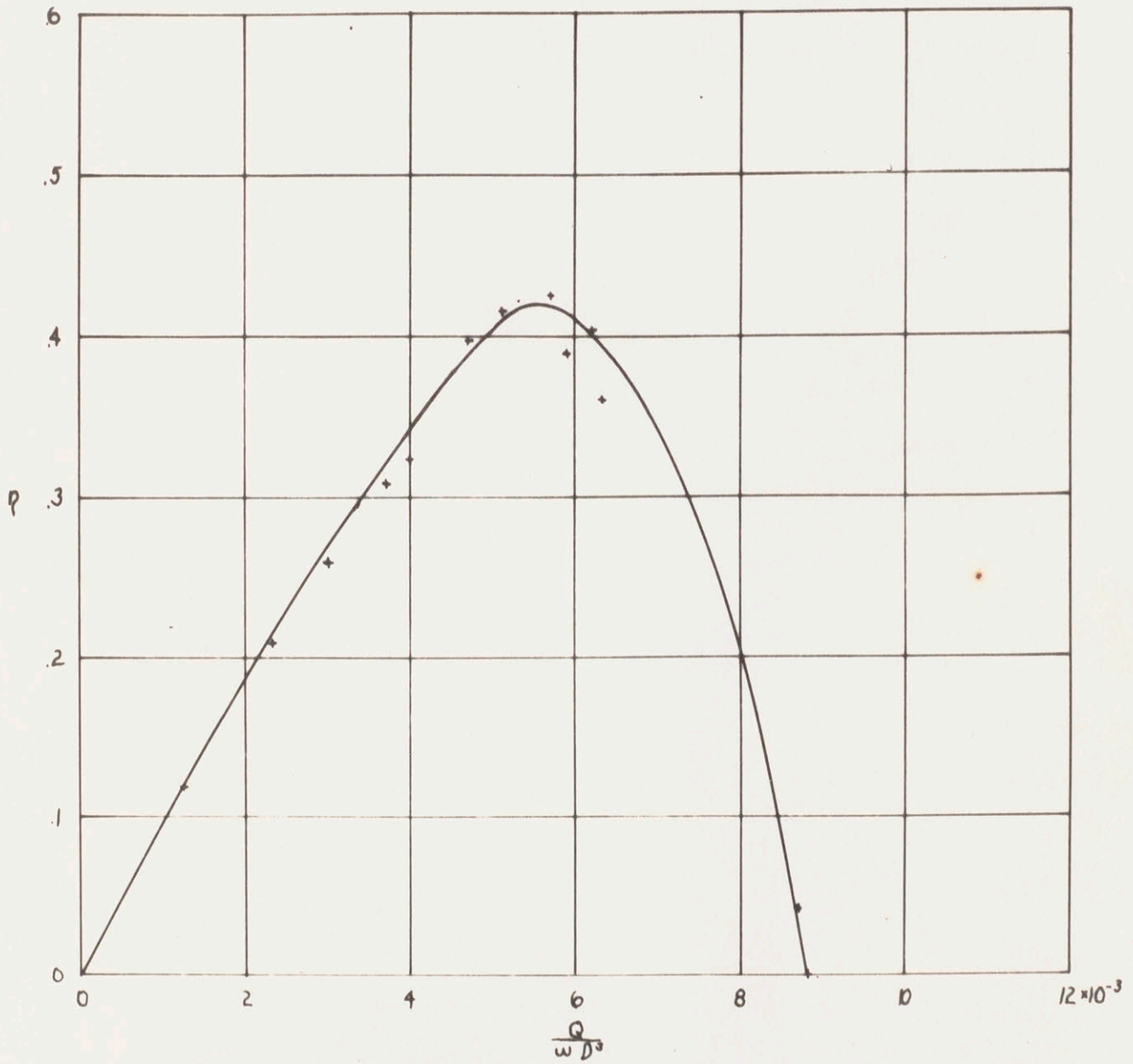

DIMENSIONLESS PLOT OF EFFICIENCY VERSUS FLOW RATE

Figures 5,6,7,8, and 9 indicate that pressure is a linear function of angle. As can be seen in Drawing "1*, the radius at 0 degrees (in line with the bolt hole) is approximately 130 degrees from the entrance to the inner surface of the head. All but two of the taps are at least 160 degrees from the exit. Therefore, we may consider that end effects are at a minimum in the tapped region. (It is singularly fortunate that the entrance to the head should fall 360 degrees from this region. In no other place could the inner and the outer taps have been installed.)

The fact that the relation between pressure and angle is indeed a linear one is conclusively demonstrated by the graph of Fig. 20. The extreme measurements for these curves are located 144 degrees apart and the relation is still linear.

It is evident that $dp/d\theta$ is a constant at all radii and for the full range of through-flows. It is also clear that the constant is different for each radii and through flow. This is what we would expect since the pressure rise across the pump decreases with increased flow.

The fact that $dp/d\theta$ is constant for each given set of conditions enables us to determine its value for corresponding points throughout the pump through simple extrapolation and indicates that flow conditions anywhere within the pump (suitably removed from entrance and exit effects) can be found if they are known for a

---

*See Descriptive Appendix

FIG. 5

STANDARD IMPELLER

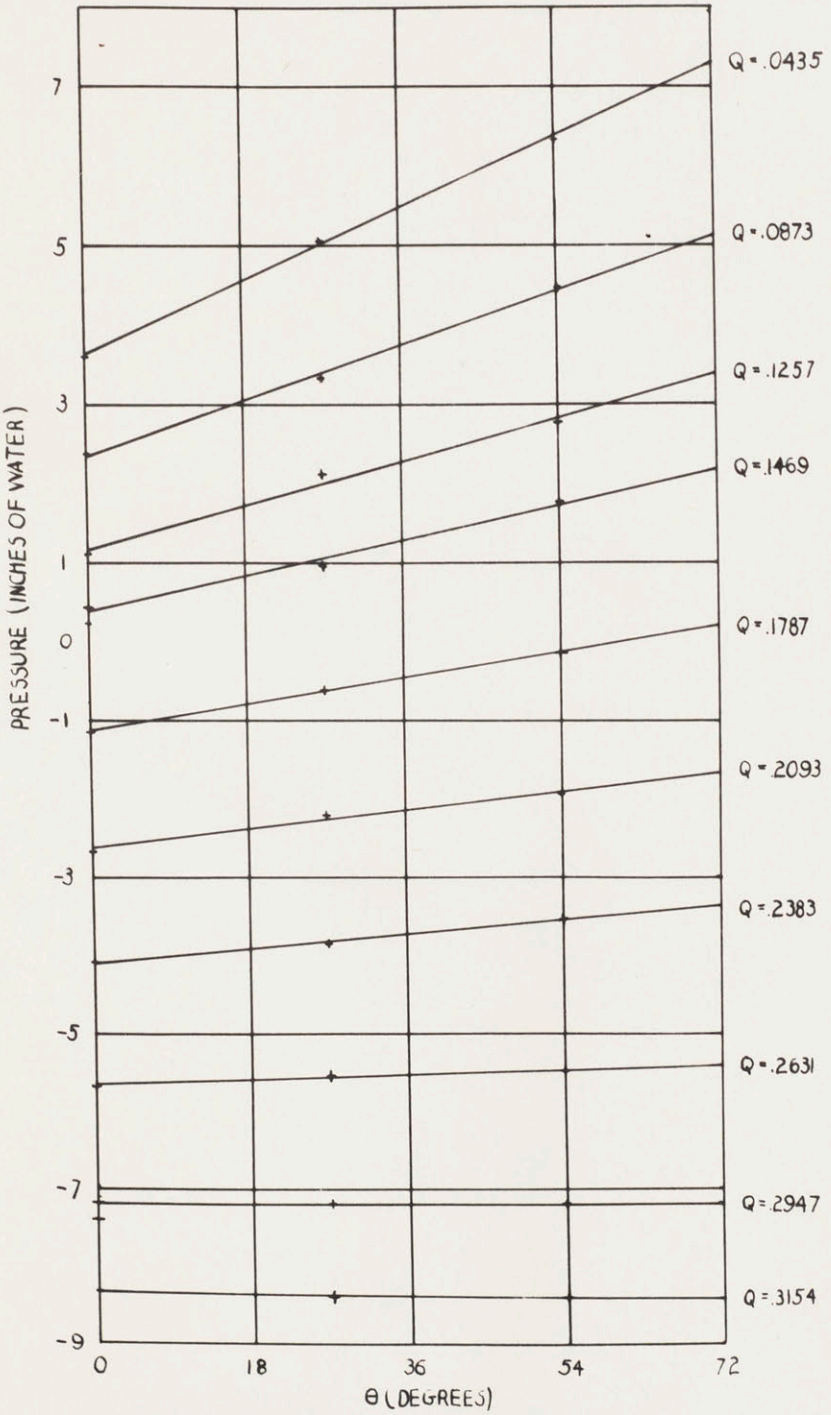

GRAPH OF PRESSURE VERSUS ANGLE AT A RADIUS OF 1.812" FOR DIFFERENT THROUGH-FLOWS (Q)(FT³/SEC OF AIR)

FIG. 6

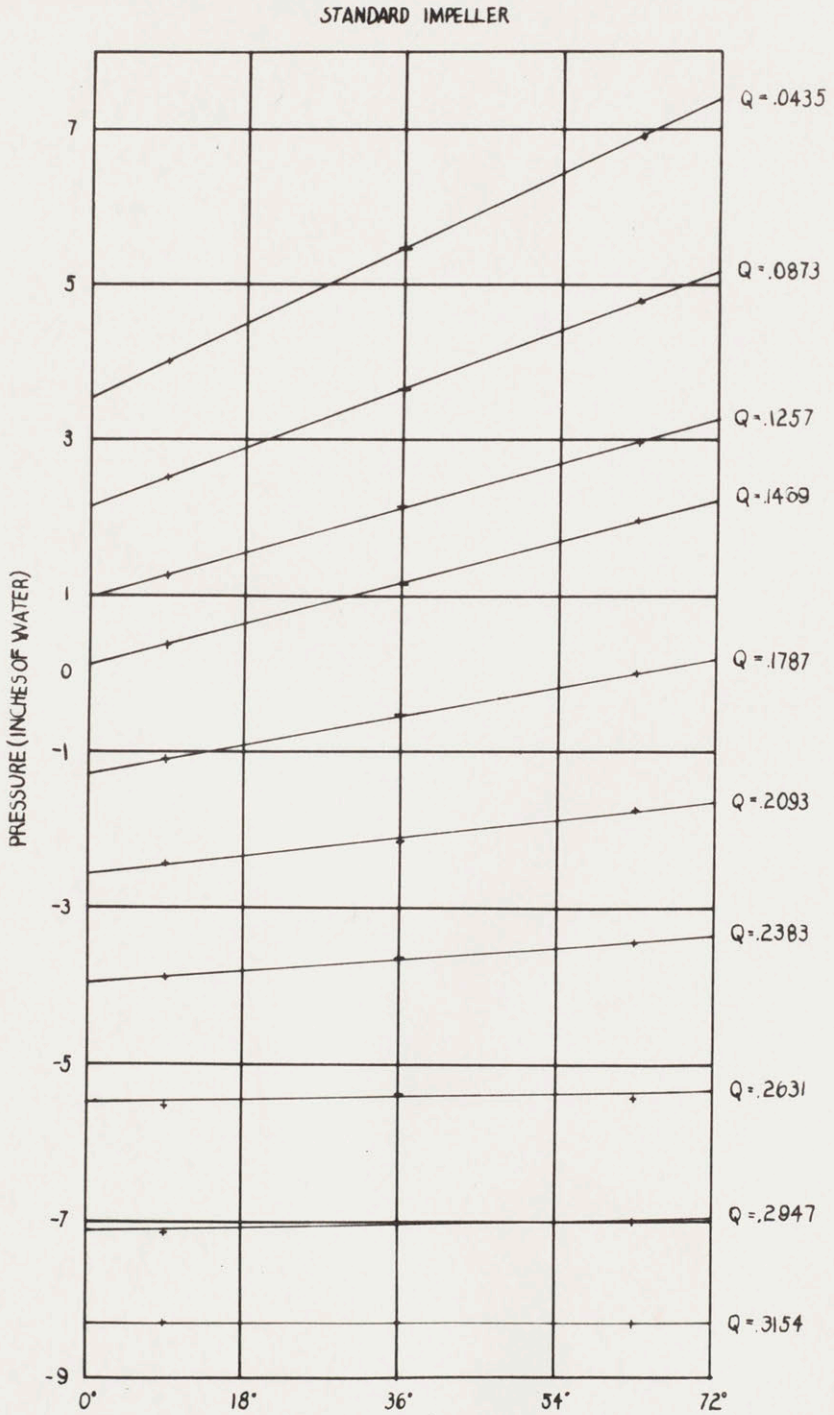

GRAPH OF PRESSURE VERSUS ANGLE AT A RADIUS OF 2.1" FOR DIFFERENT THROUGH-FLOWS (Q)(FT^3/SEC OF AIR)

FIG. 7

STANDARD IMPELLER

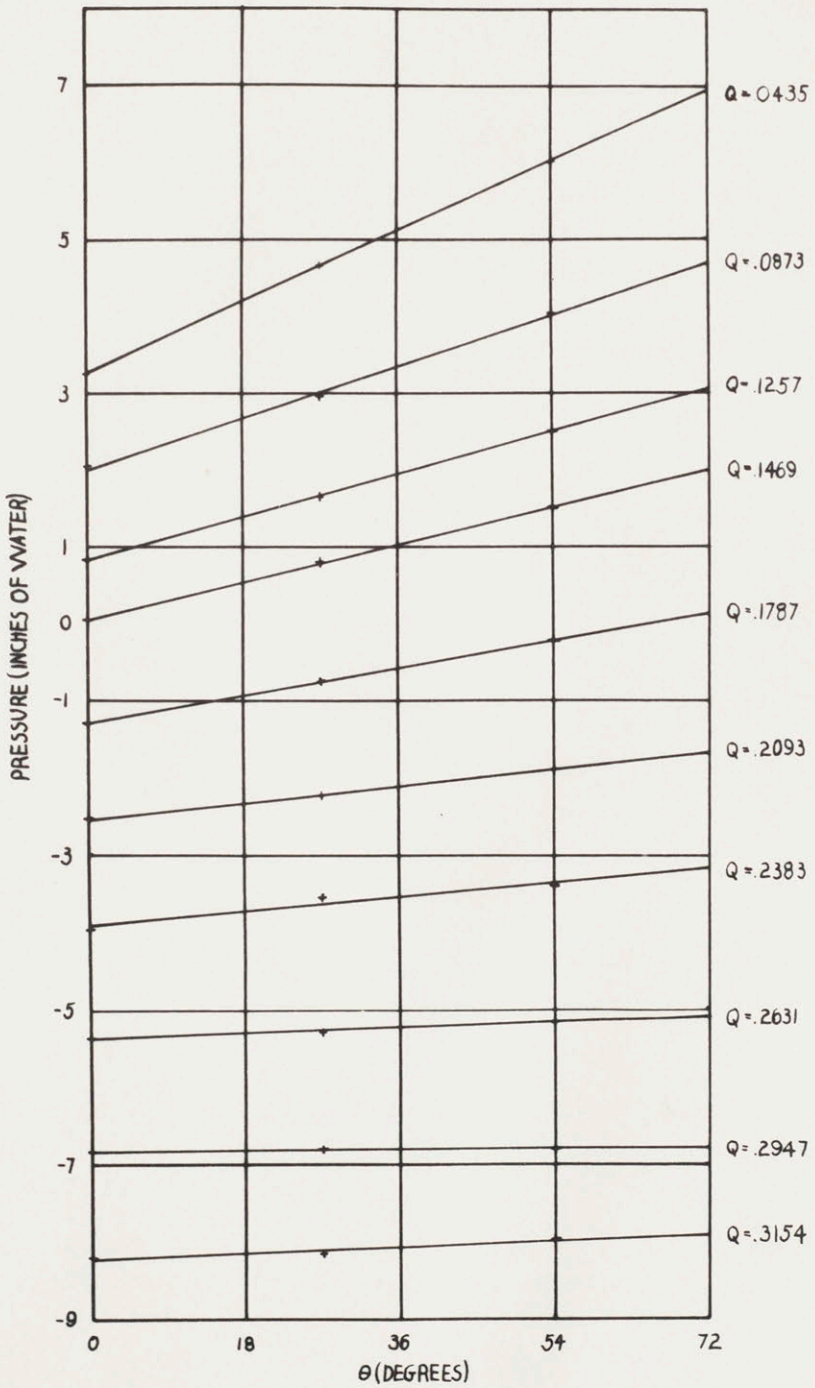

GRAPH OF PRESSURE VERSUS ANGLE AT A RADIUS OF 2.4" FOR DIFFERENT THROUGH-FLOWS (Q) (FT³/SEC OF AIR)

FIG. 8

STANDARD IMPELLER

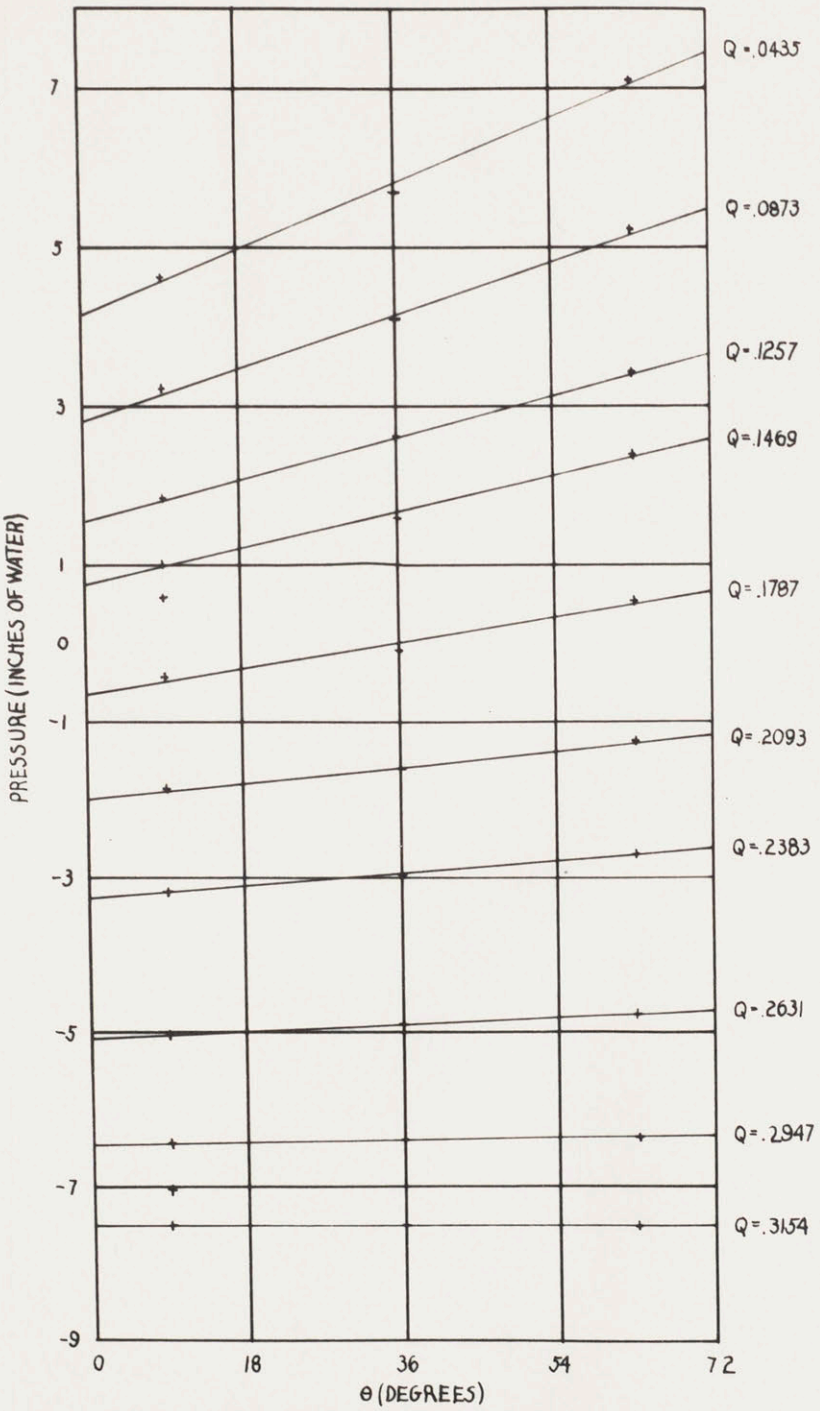

GRAPH OF PRESSURE VERSUS ANGLE AT OUTER RADIUS OF 2.88"
FOR DIFFERENT THROUGH-FLOWS (Q)(FT³/SEC OF AIR)

FIG. 9

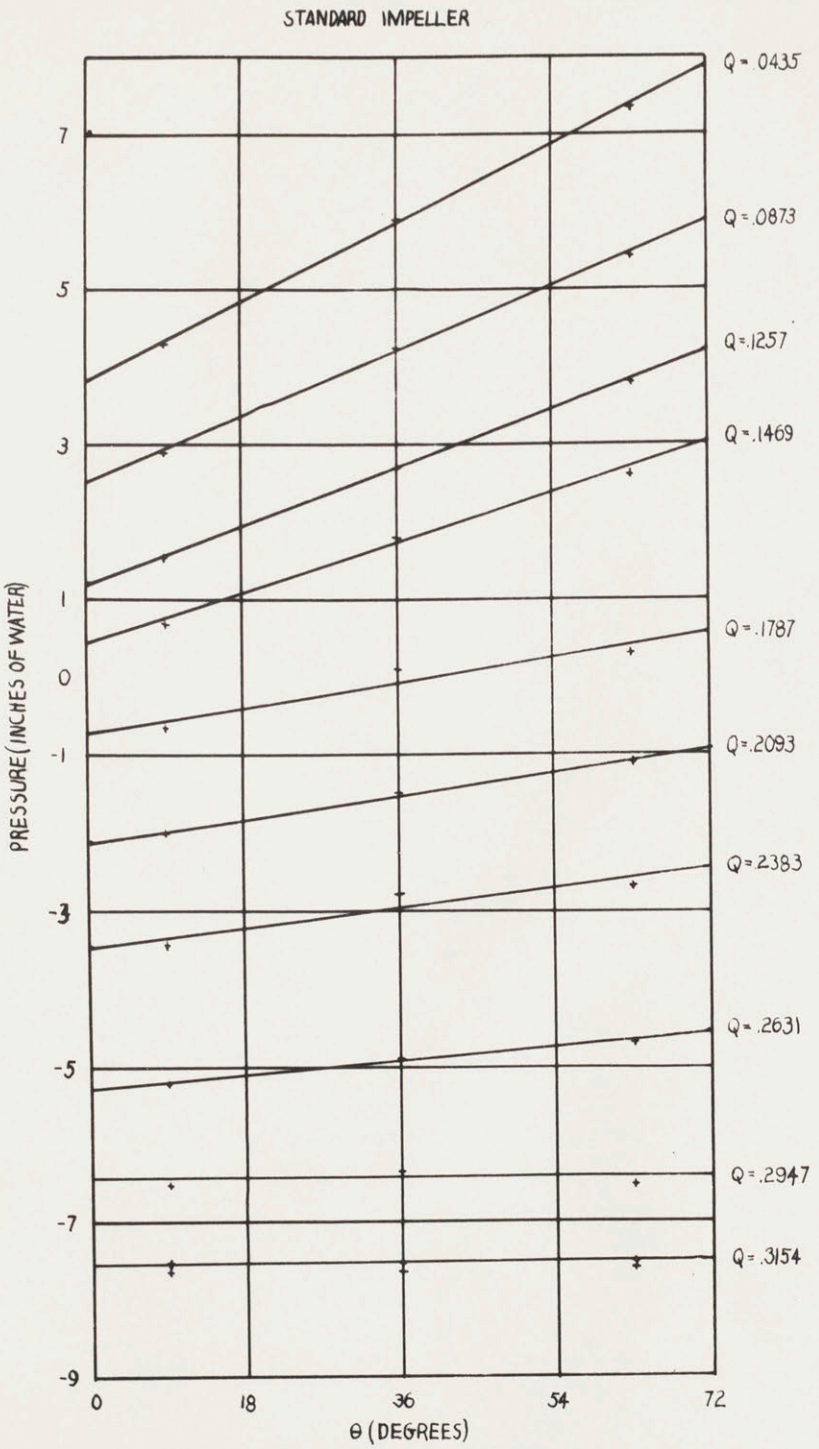

GRAPH OF PRESSURE VERSUS ANGLE AT INNER RADIUS OF 2.88"
FOR DIFFERENT THROUGH-FLOWS (Q)(FT^3/SEC OF AIR)

STANDARD IMPELLER

FIG. 20

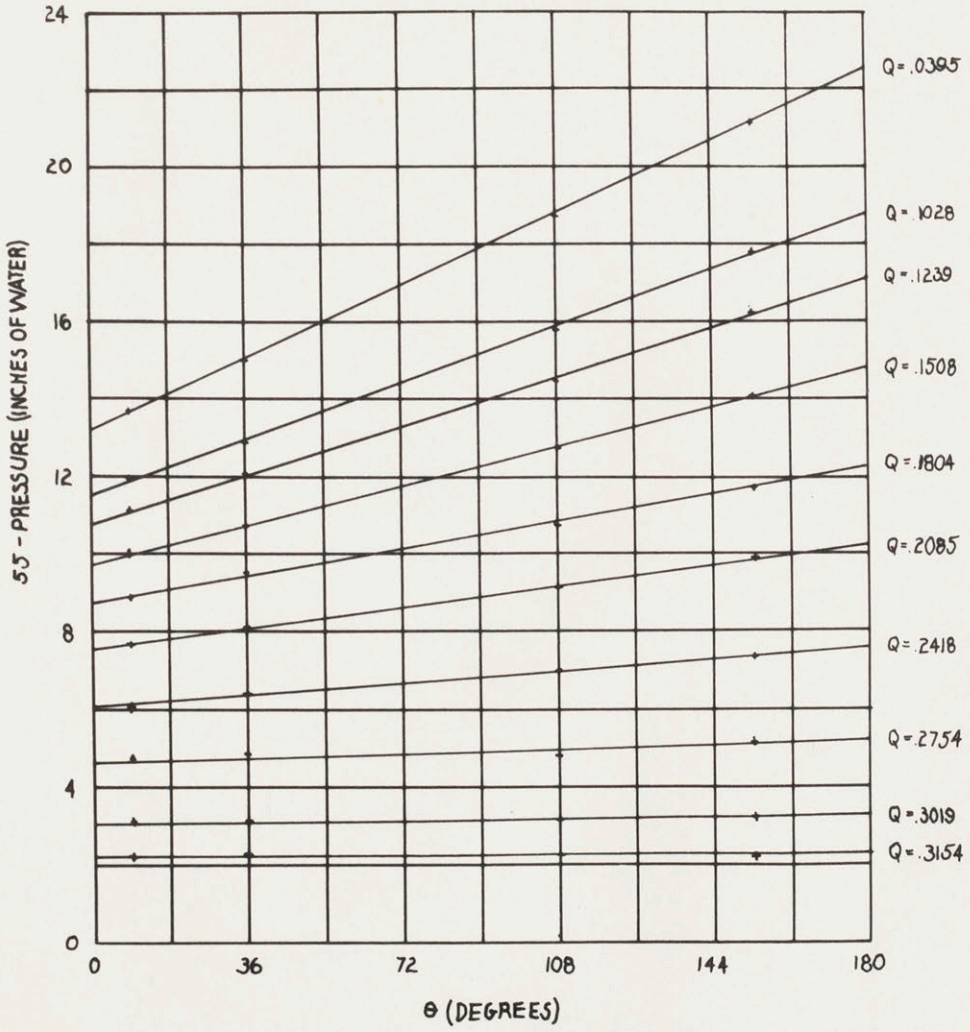

GRAPH OF PRESSURE VERSUS ANGLE AT A RADIUS OF 2.1" FOR DIFFERENT THROUGH-FLOWS (Q)(FT³/SEC OF AIR)

given cross section.

In Fig. 10, $dp/d\theta$'s for different radii are plotted for different through-flows. The most surprising fact to come from this graph is that the curves of radii 1.812", 2.1", and 2.4" very nearly coincide. We may therefore state that at these radii $dp/d\theta$ varies only with the through-flow. As can be seen in Drawing #4*, the holes at these radii are located where the streamline curvature is likely to be the smallest. It is significant that the gaps between the three closely grouped curves and the two flanking them, decrease with increasing through-flow. The convergence of these curves might be construed to indicate that the effect of streamline curvature decreases with increasing through-flow. We shall see later on that this is probably the case.

In order to discuss intelligently the graphs of pressure versus radius presented in Fig. 11, we should first consider qualitatively the flow through the pump. In Drawing #5, the two general types of velocity components are illustrated. There are two types of flow within the pump: first, there is the circulatory flow, Q_c, caused by the recirculation of the fluid through the teeth of the impeller; second, there is the through-flow, Q, or the tangential flow through the pump. In the drawing, the velocity components of these flows are schematically sketched without consideration of friction, boundary ef-

---

*See Descriptive Appendix

FIG. 10

STANDARD IMPELLER

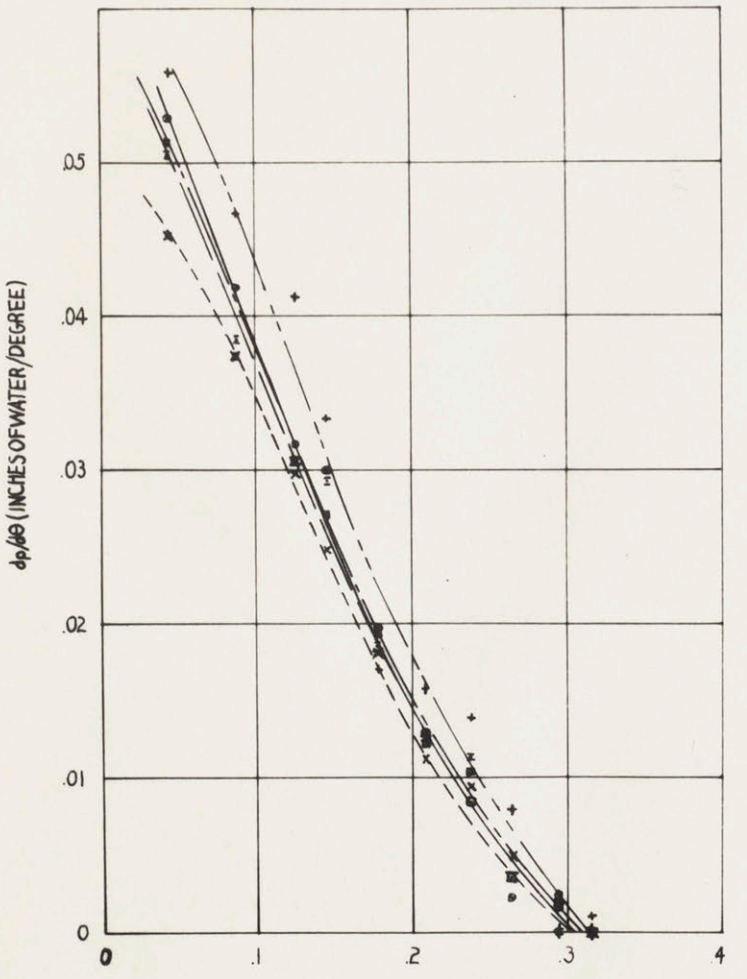

GRAPH OF dp/dθ VERSUS THROUGH-FLOW FOR DIFFERENT RADII

TANGENTIAL VELOCITY COMPONENTS
FOR DIFFERENT THROUGH-FLOWS (Q) CONST. SPEED

CIRCULATORY FLOW PATTERN

M.E. DEPT. M.I.T.		STA-RITE REGENERATIVE PUMP	TH-7
G. F. LUTZ	MAY 25, 1953	SKETCH OF FLOW PATTERNS	5

fects, etc. A three dimensional combination of these components would yield a circumferential helix.

At low flow rates in this pump there is also some tangential recirculation. As the flow is increased, the tangential recirculation diminishes and finally disappears. If we can prove that solid body rotation occurs at very high flow rates ($dp/d\theta = 0$), we will have demonstrated that not only that the tangential recirculation has ceased, but also that the circulatory flow is equal to zero. Such proof may be used to establish end conditions for the theoretical formulae.

For this reason, and to learn something about dp/dr, the graphs of Fig. 11 were plotted. Since $dp/d\theta$ is independent of radius where dp/dr is equal to zero, we could also determine the points at which this condition occurs.

If we have solid body rotation, the pressure will follow the relation: $p = \rho w^2 r^2/2$. If we solve this expression* for r equal to 1.812" and 2.88" we obtain pressures respectively equal to 3.73 and 9.39 lbs/ft^2. The pressure difference measured** is equal to about .95 " of water. If we convert the theoretical pressure difference to inches of water we obtain a value of 1.09". The error between the two is only .14", well within the estimated error of .2". It seems reasonable to conclude that we have here solid body rotation.

---

* See Calculations Appendix

**At Q equal to .3154 ft^3/sec, $dp/d\theta$ equal to zero.

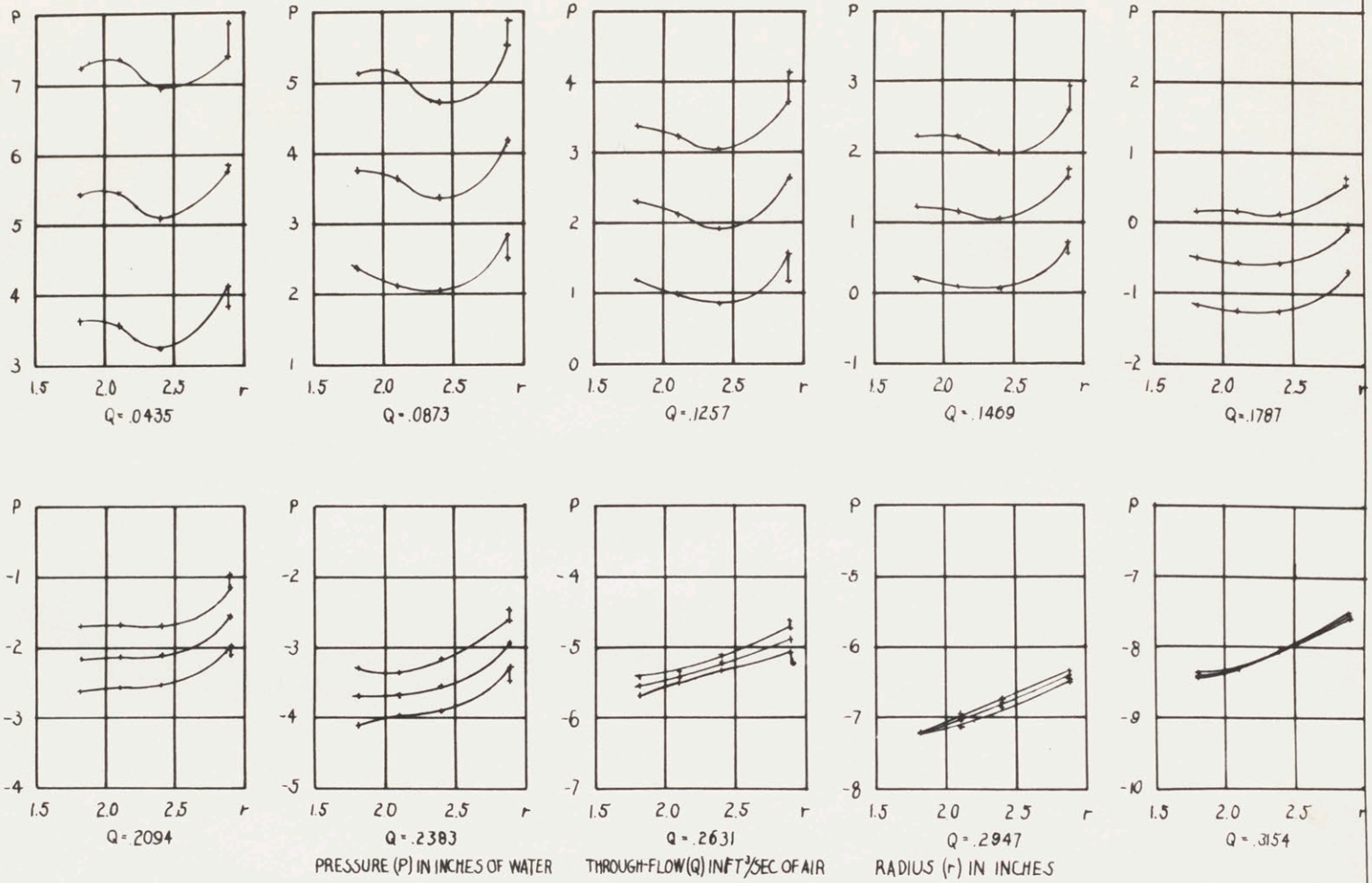

GRAPHS OF PRESSURE VERSUS RADIUS AT THREE ANGLES FOR DIFFERENT THROUGH-FLOWS

UPPER CURVES: $\theta = 72°$ MIDDLE CURVES: $\theta = 36°$ LOWER CURVES: $\theta = 0°$

STANDARD IMPELLER

FIG 11

If we have solid body rotation, the pressure is a function of radius only, assuming that density and angular velocity are constant. Accordingly, we should expect that the curves of pressure versus radius for different values of θ should coincide when this condition exists. As can be seen on the last graph of Fig. 11, approximate coincidence is achieved.

It seems probable that the increasing spread between the different curves as the through-flow is reduced may be a measure of the circulatory flow. Further conclusions regarding this matter must await quantitative velocity measurements.

It is clear that dp/dr is not a constant, but a rather complicated function. Only when Q is equal to .2094 ft^3/sec does it remain near zero for any length of time.

It should be noted that the last point on each curve behaves in a very erratic manner. I can offer no really satisfactory reason for its behavior. However, since this tap is located almost directly over the center of the impeller blade and receives the full force of the circulatory flow, it may be considered as giving less reliable readings than the others. If we assume that these eccentric readings are caused by the circulatory flow, we should expect the eccentricity to diminish with this flow. The fact that it does diminish and eventually disappears is partial verification of this hypothesis.

Figures 12 through 19 contain the same information on pressure previously discussed, for another test run. In every case they are consistent with that obtained from the run discussed. They are included here in order to substantiate further the conclusions drawn.

FIG. 12

STANDARD IMPELLER

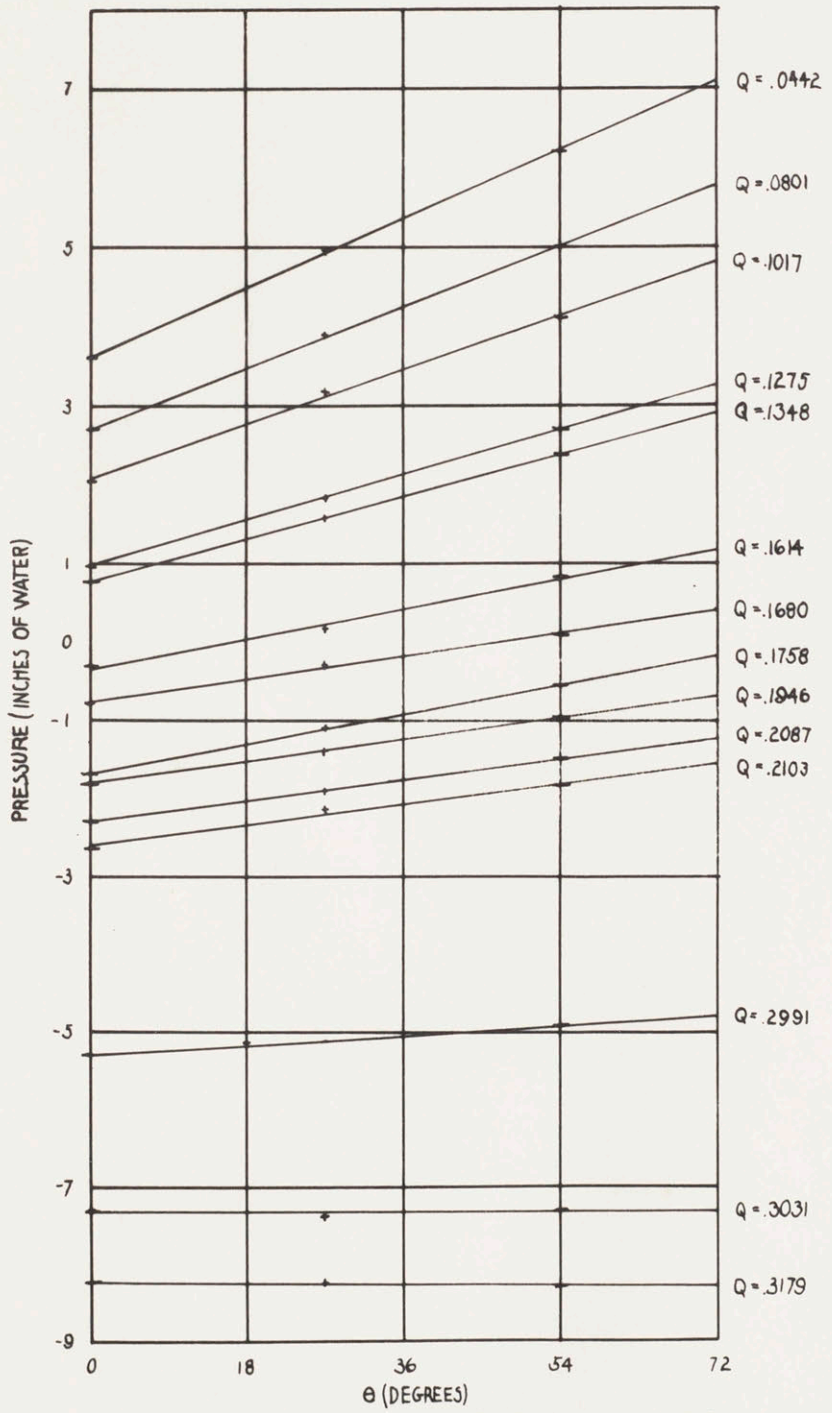

GRAPH OF PRESSURE VERSUS ANGLE AT A RADIUS OF 1.812" FOR DIFFERENT THROUGH-FLOWS (Q)(FT³/SEC OF AIR)

FIG. 13

STANDARD IMPELLER

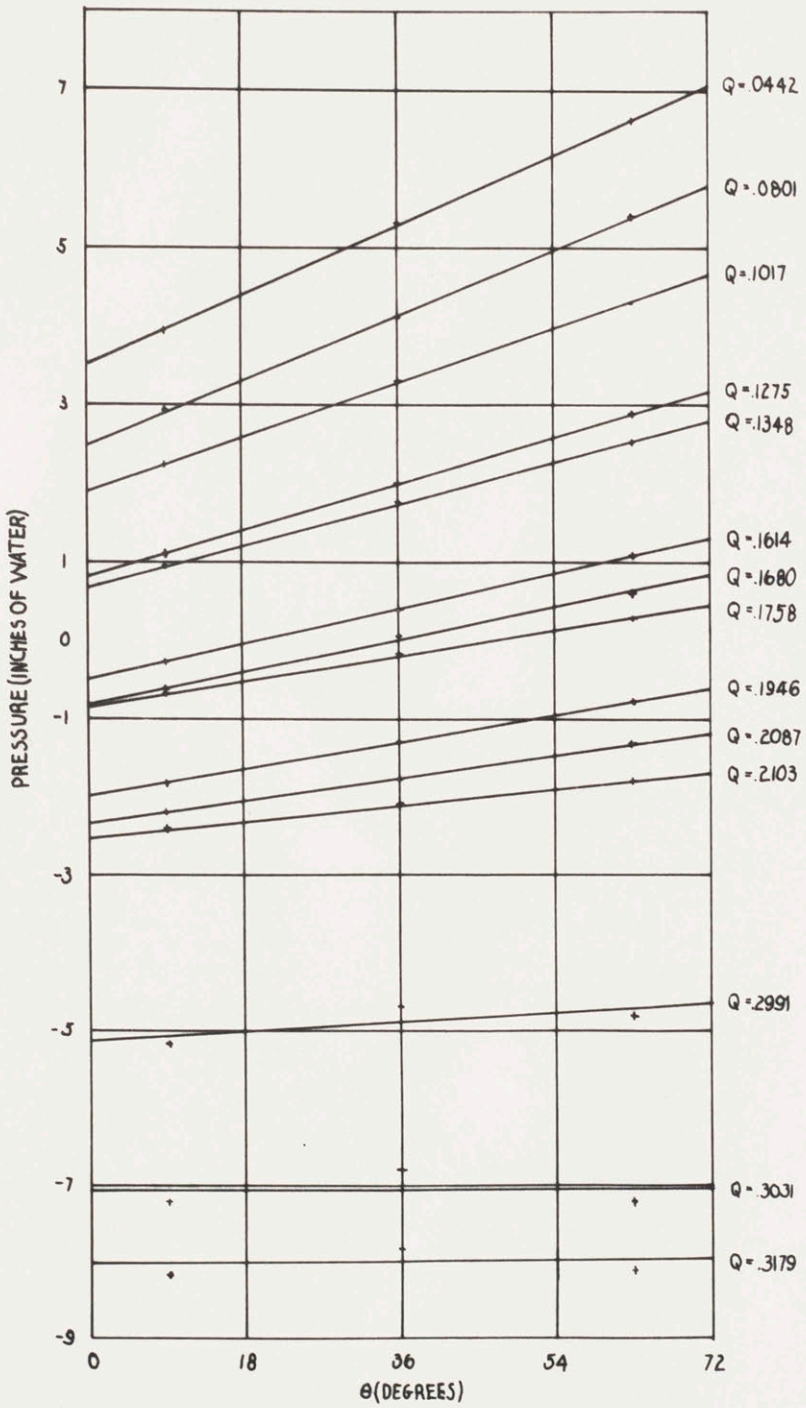

GRAPH OF PRESSURE VERSUS ANGLE AT A RADIUS OF 2.1" FOR DIFFERENT THROUGH-FLOWS (Q)(FT³/SEC OF AIR)

FIG. 14

STANDARD IMPELLER

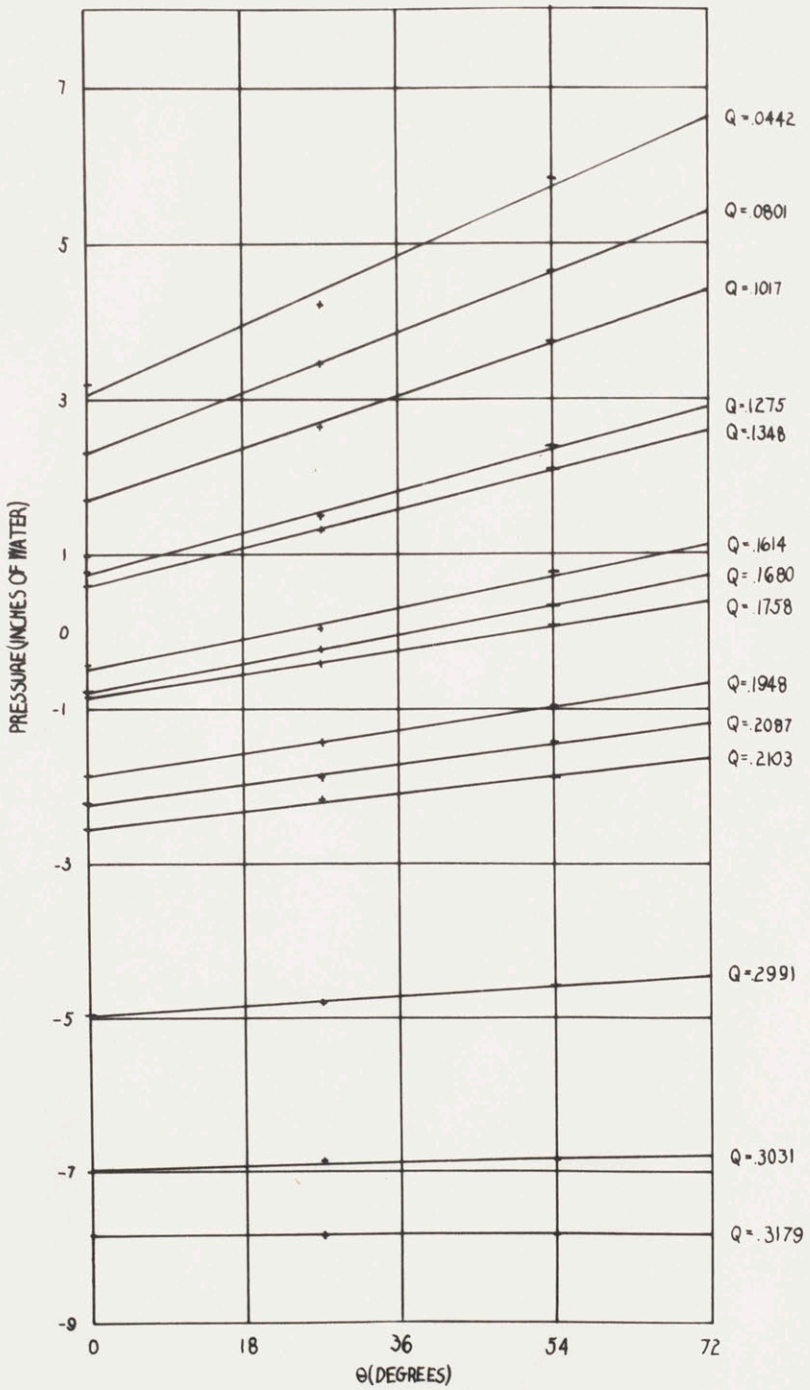

GRAPH OF PRESSURE VERSUS ANGLE AT A RADIUS OF 2.4" FOR DIFFERENT THROUGH-FLOWS (Q) (FT³/SEC OF AIR)

FIG. 15

STANDARD IMPELLER

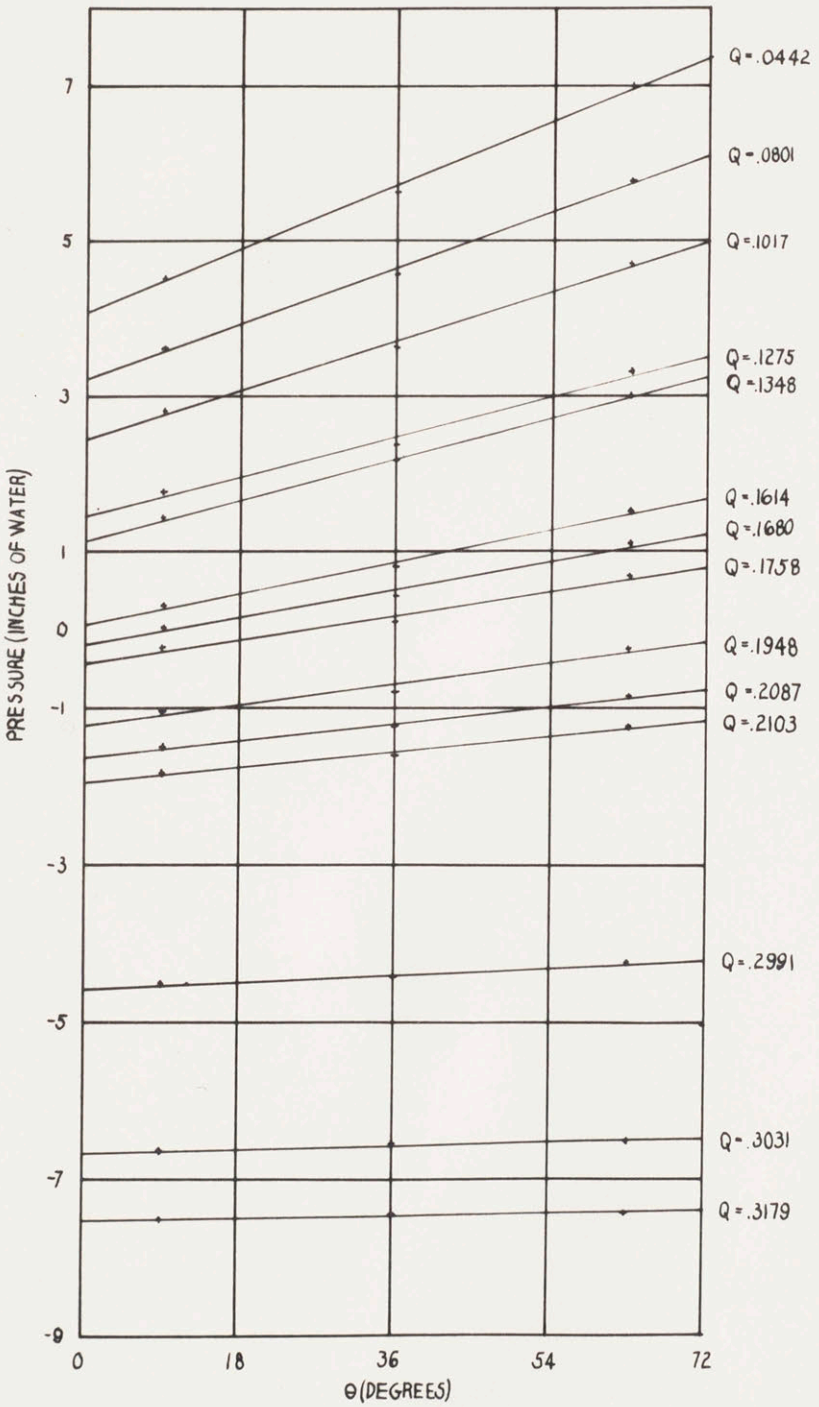

GRAPH OF PRESSURE VERSUS ANGLE AT OUTER RADIUS OF 2.88" FOR DIFFERENT THROUGH-FLOWS (Q)(FT^3/SEC OF AIR)

FIG. 16

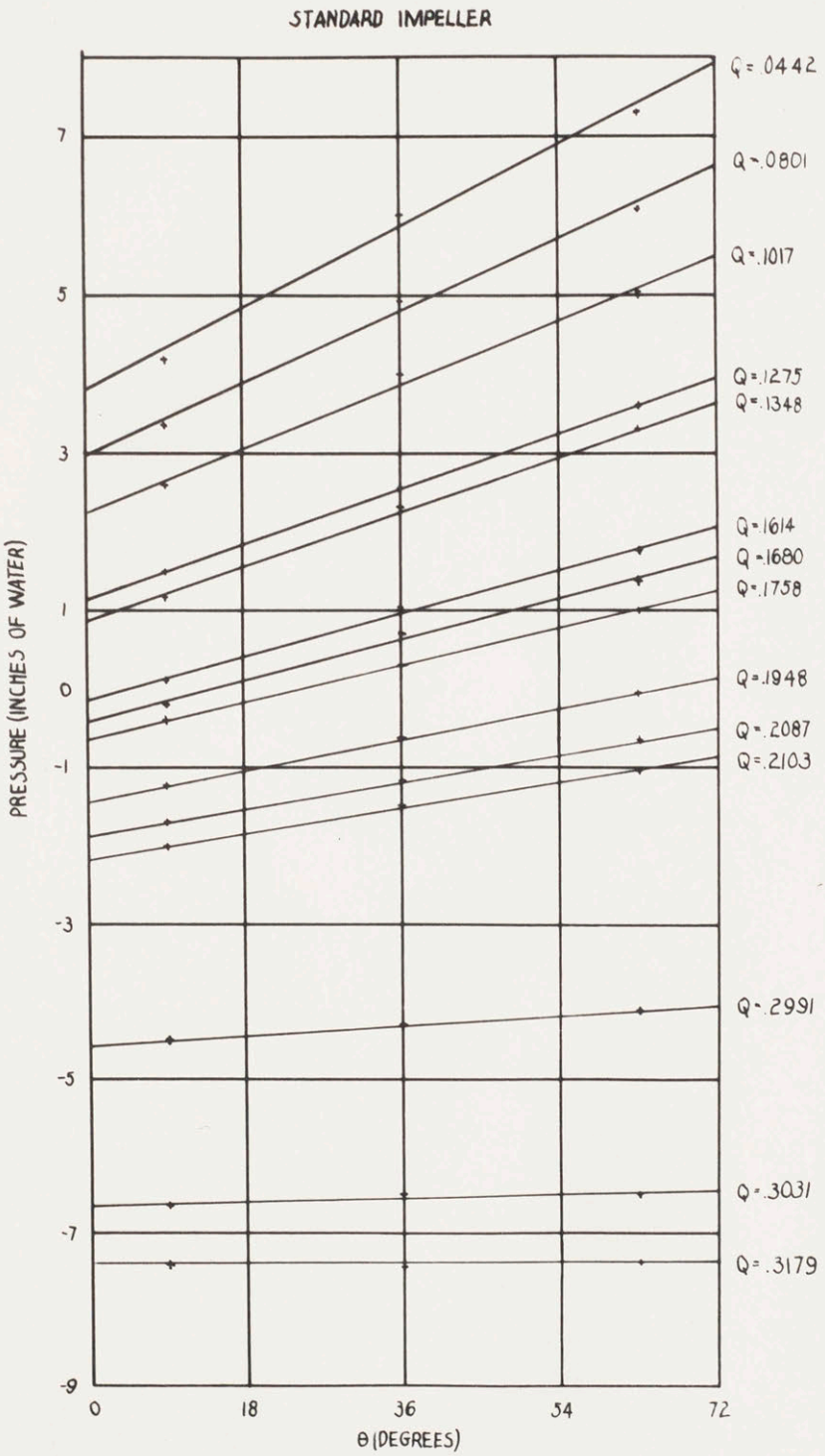

GRAPH OF PRESSURE VERSUS ANGLE AT INNER RADIUS OF 2.88" FOR DIFFERENT THROUGH-FLOWS (Q)(FT^3/SEC OF AIR)

FIG. 17

STANDARD IMPELLER

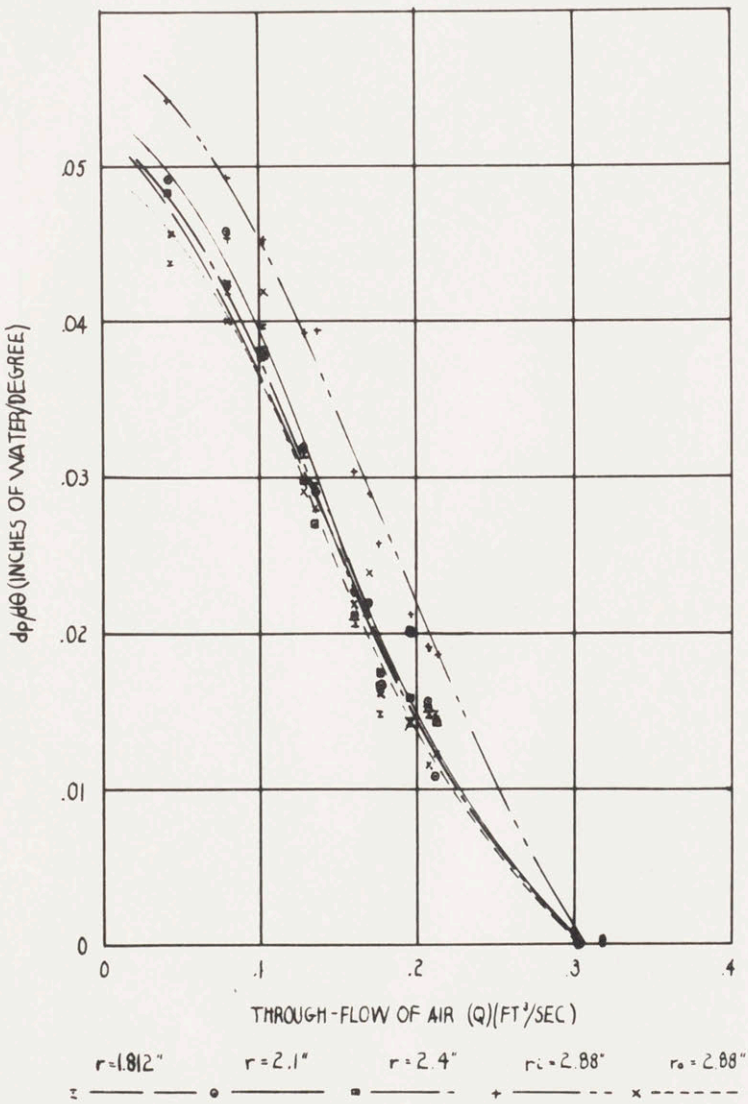

GRAPH OF dp/dθ VERSUS THROUGH-FLOW FOR DIFFERENT RADII

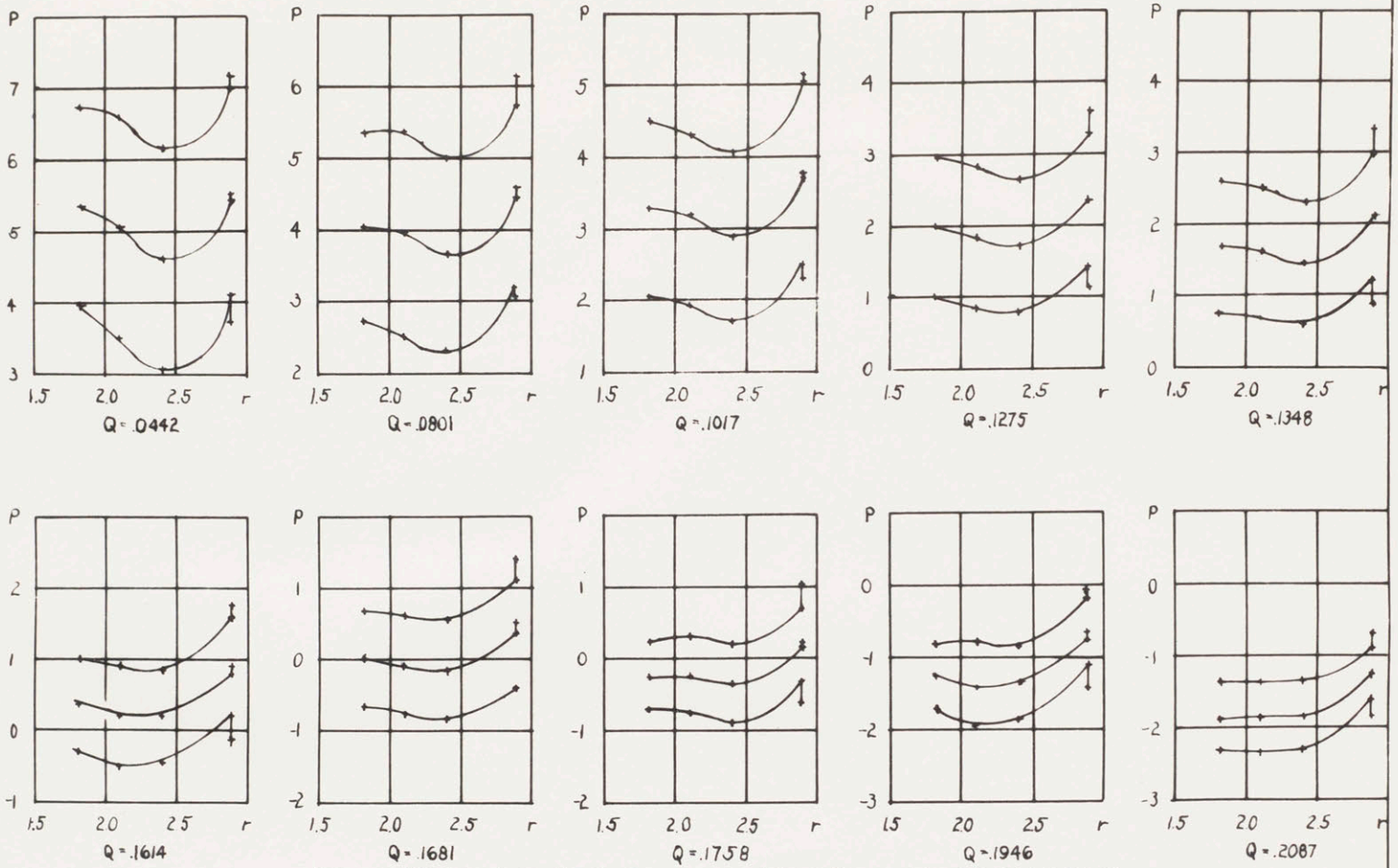

PRESSURE (P) IN INCHES OF WATER THROUGH-FLOW (Q) IN FT^3/SEC OF AIR RADIUS (r) IN INCHES

GRAPHS OF PRESSURE VERSUS RADIUS AT THREE ANGLES FOR DIFFERENT THROUGH-FLOWS
UPPER CURVES: $\theta = 63°$ MIDDLE CURVES: $\theta = 31.5°$ LOWER CURVES: $\theta = 0$

STANDARD IMPELLER

FIG. 18

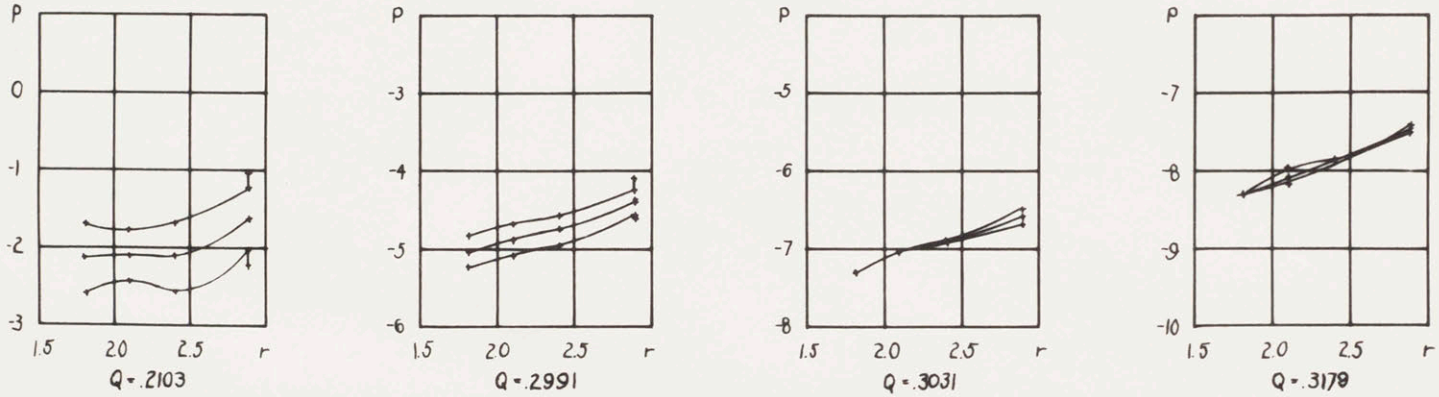

PRESSURE (P) IN INCHES OF WATER THROUGH-FLOW (Q) IN FT³/SEC OF AIR
RADIUS (r) IN INCHES

GRAPHS OF PRESSURE VERSUS RADIUS AT THREE ANGLES FOR DIFFERENT THROUGH-FLOWS
UPPER CURVES : $\theta = 63$ MIDDLE CURVES: $\theta = 31.5°$ LOWER CURVES: $\theta = 0°$

STANDARD IMPELLER

FIG. 19

Shrouded Impeller

The data compiled from the experiment with the shrouded rotor* will not be discussed in detail. The throttling effect of friction was much greater than had been expected and the efficiency and head-rise across the pump were both much less than that for the standard impeller.

The data has been graphed because of its possible value to the development of the theory of flow in the pump. When more complete information on the circulatory flow is available, the shroud may be re-designed to eliminate the sharp edge of the passage, and to cut down the interference with the natural flow. Even in such a modified form it is doubtful whether the head rise obtainable will ever compare favorable to that of the pump using the standard impeller. Certainly the increased friction from the shroud will always keep the efficiency lower than that obtainable with the standard impeller.

---

* See Drawing #3 and Plate 3, Descriptive Appendix

FIG. 21

SHROUDED IMPELLER

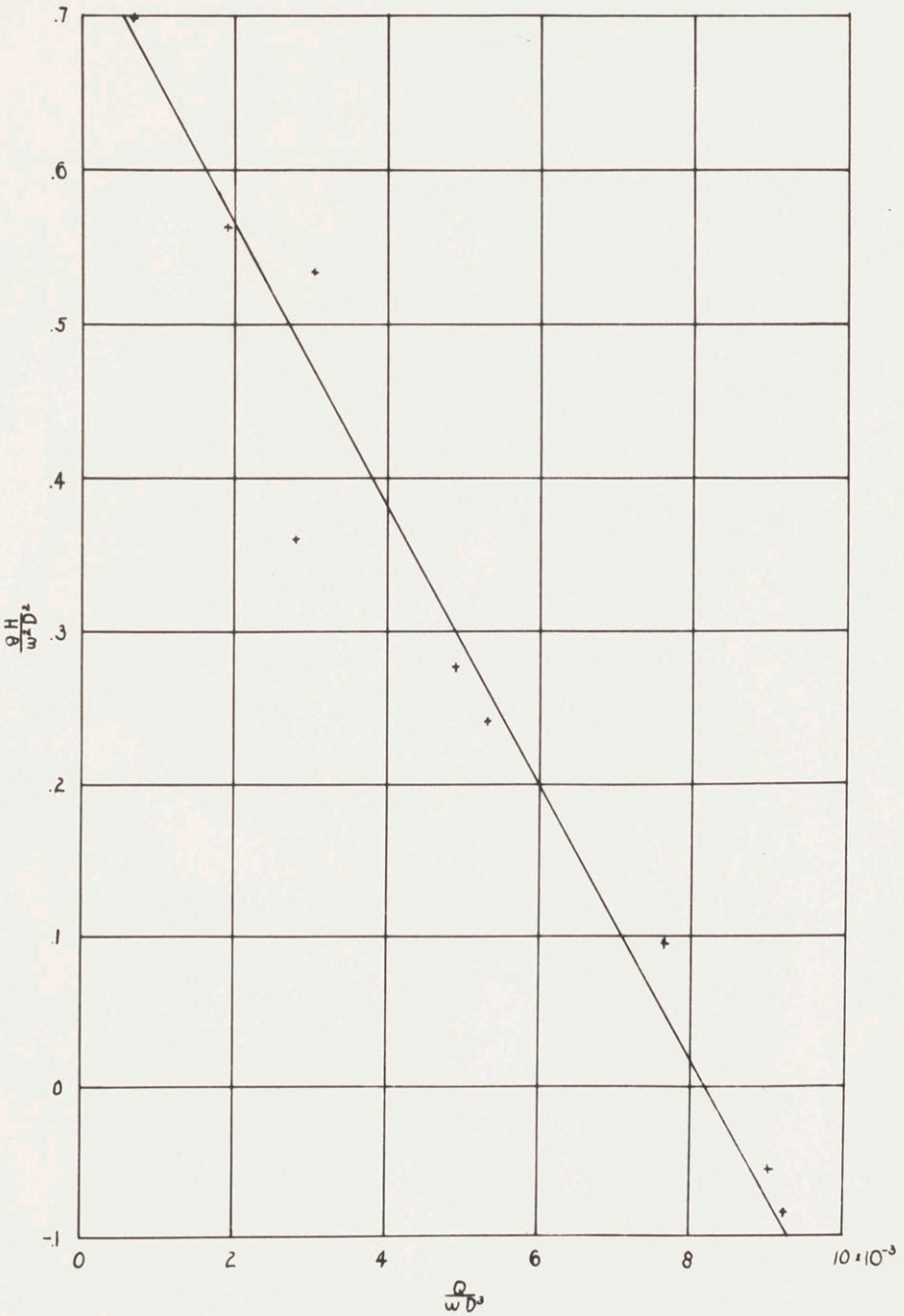

DIMENSIONLESS PLOT OF HEAD VERSUS THROUGH-FLOW RATE

SHROUDED IMPELLER

FIG. 22

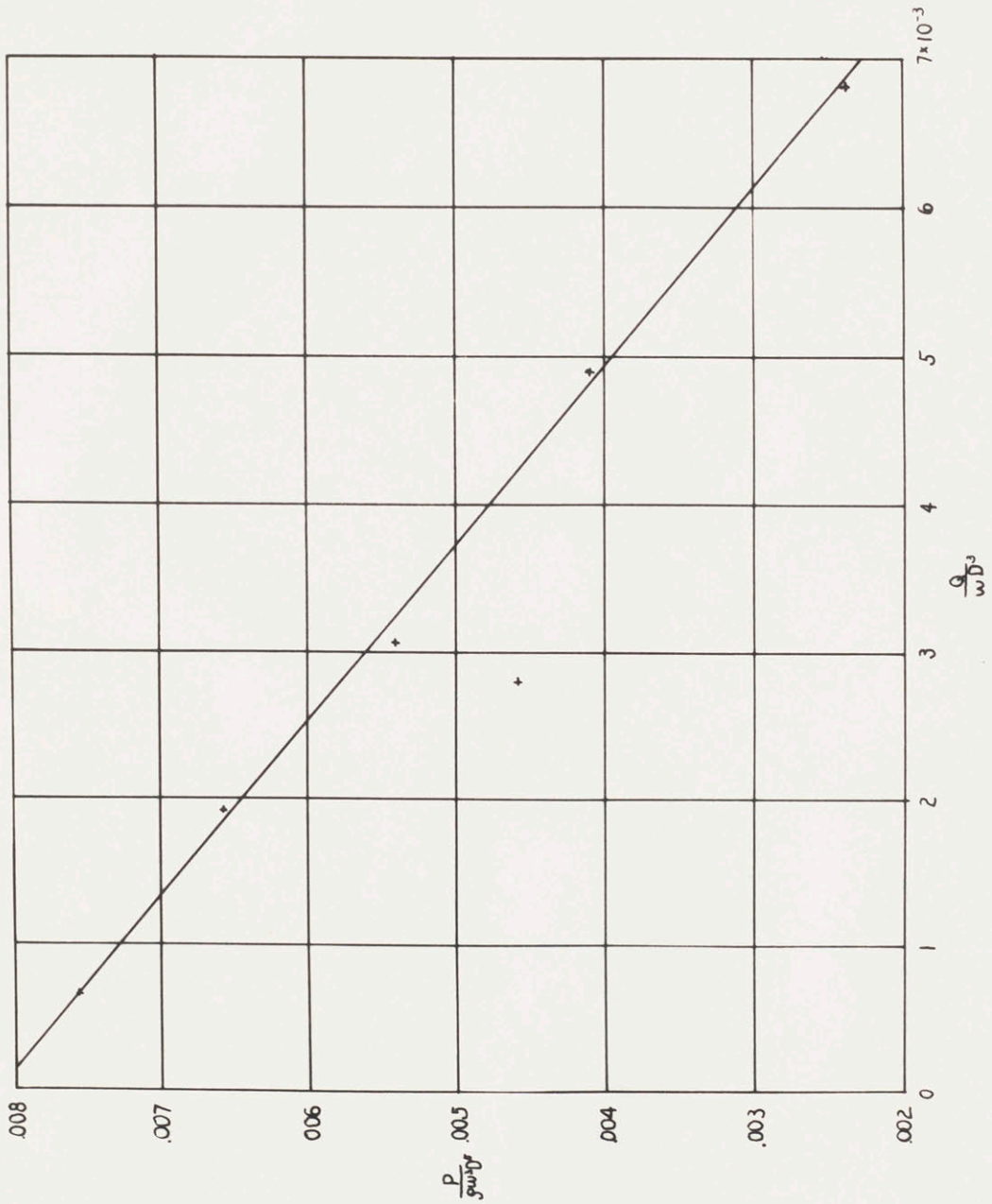

DIMENSIONLESS PLOT OF POWER (BRAKE) VERSUS THROUGH-FLOW RATE

FIG 23

SHROUDED IMPELLER

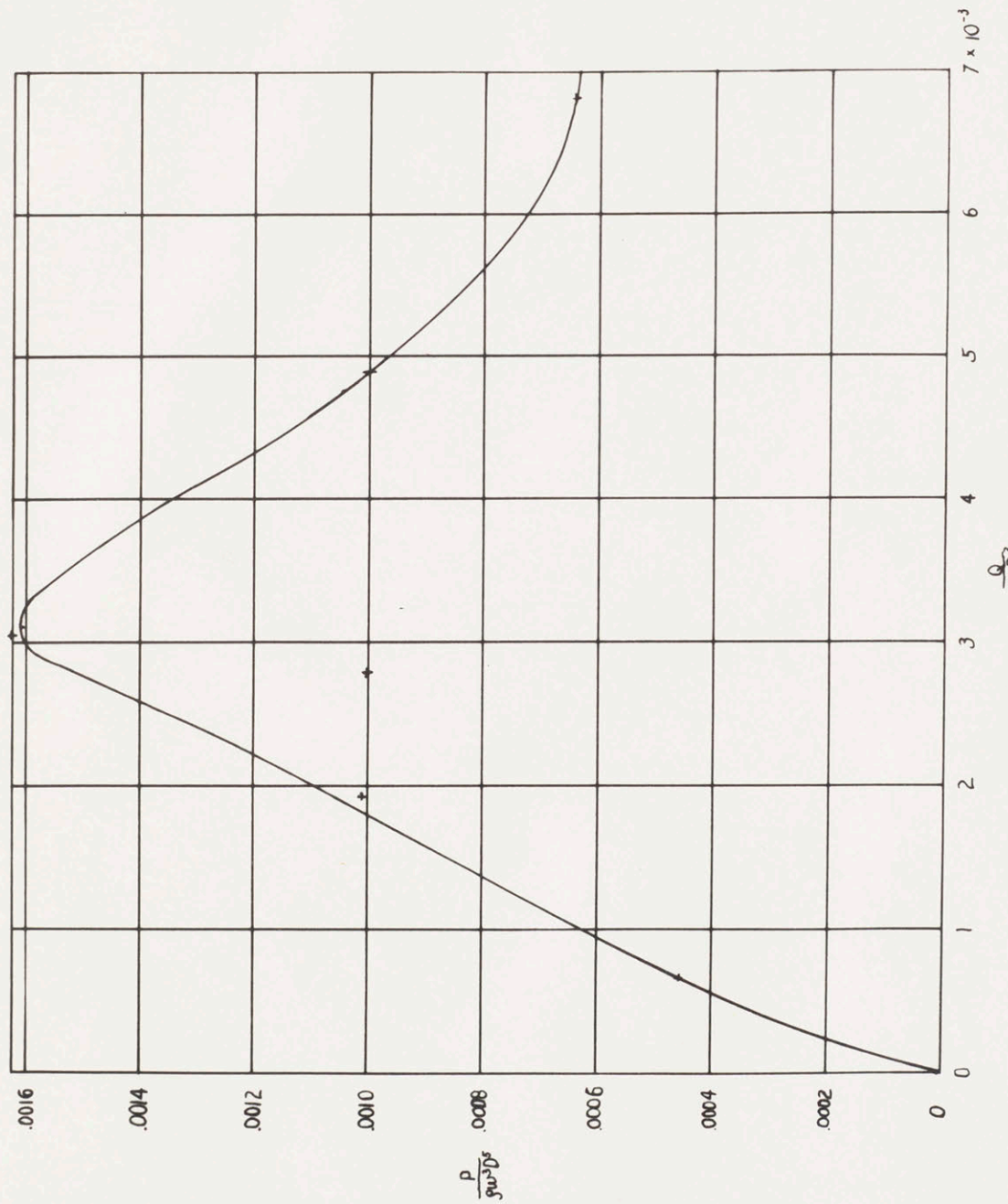

DIMENSIONLES PLOT OF POWER (USEFUL) VERSUS THROUGH-FLOW RATE

FIG. 24

SHROUDED IMPELLER

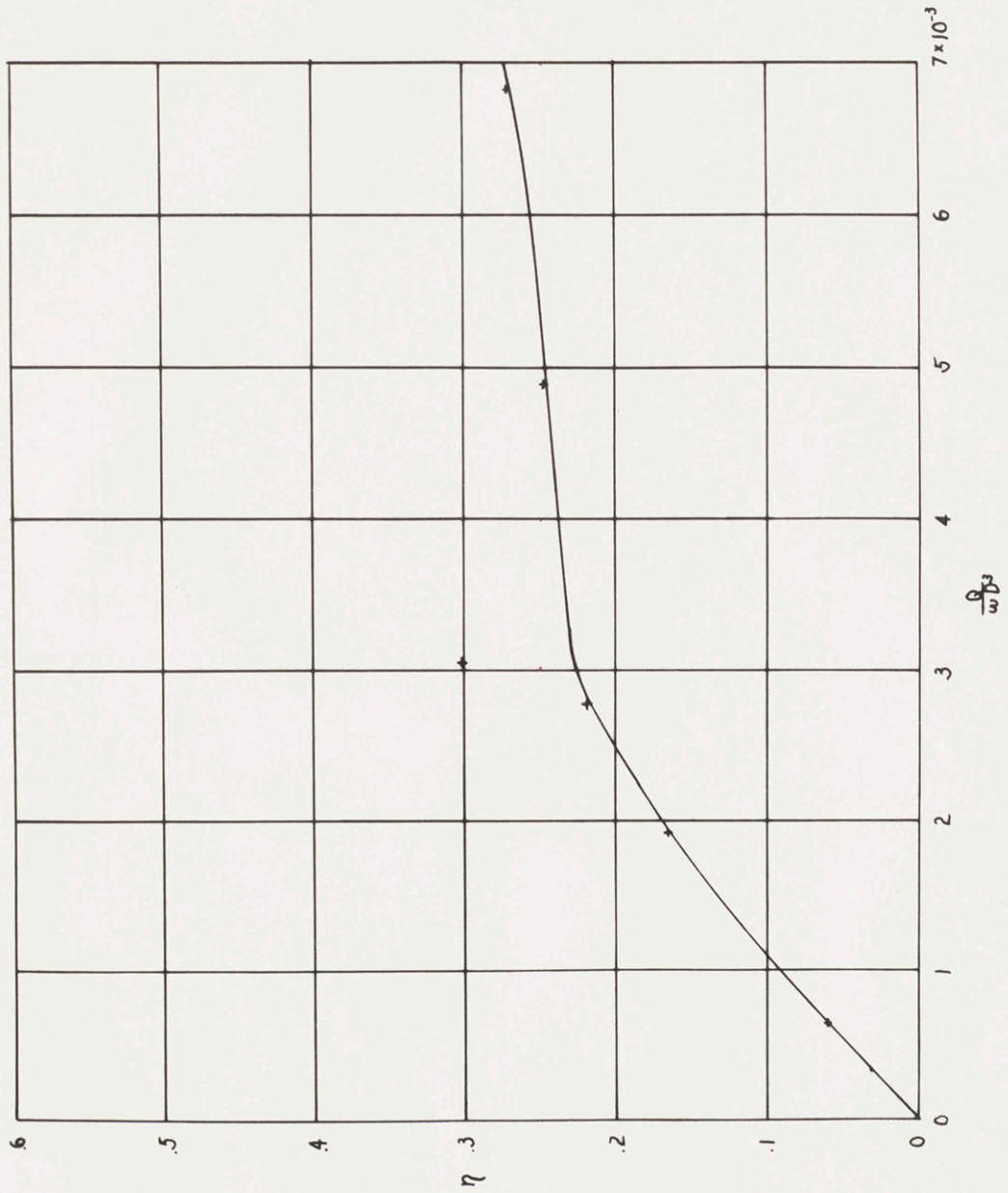

DIMENSIONLESS PLOT OF EFFICIENCY VERSUS THROUGH-FLOW RATE

FIG. 24A

SHROUDED IMPELLER

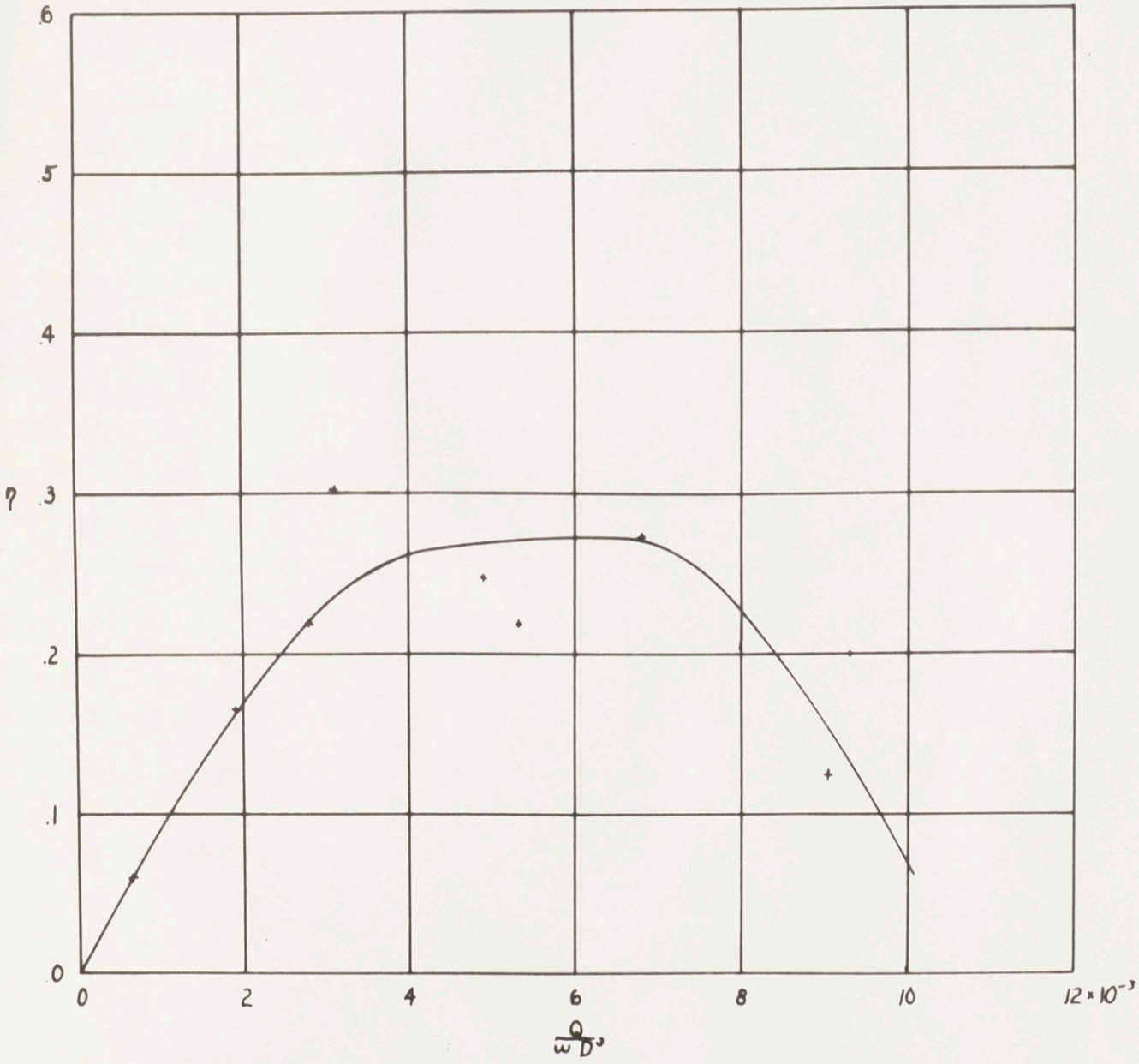

DIMENSIONLESS PLOT OF EFFICIENCY VERSUS THROUGH-FLOW

SHROUDED IMPELLER

FIG. 25

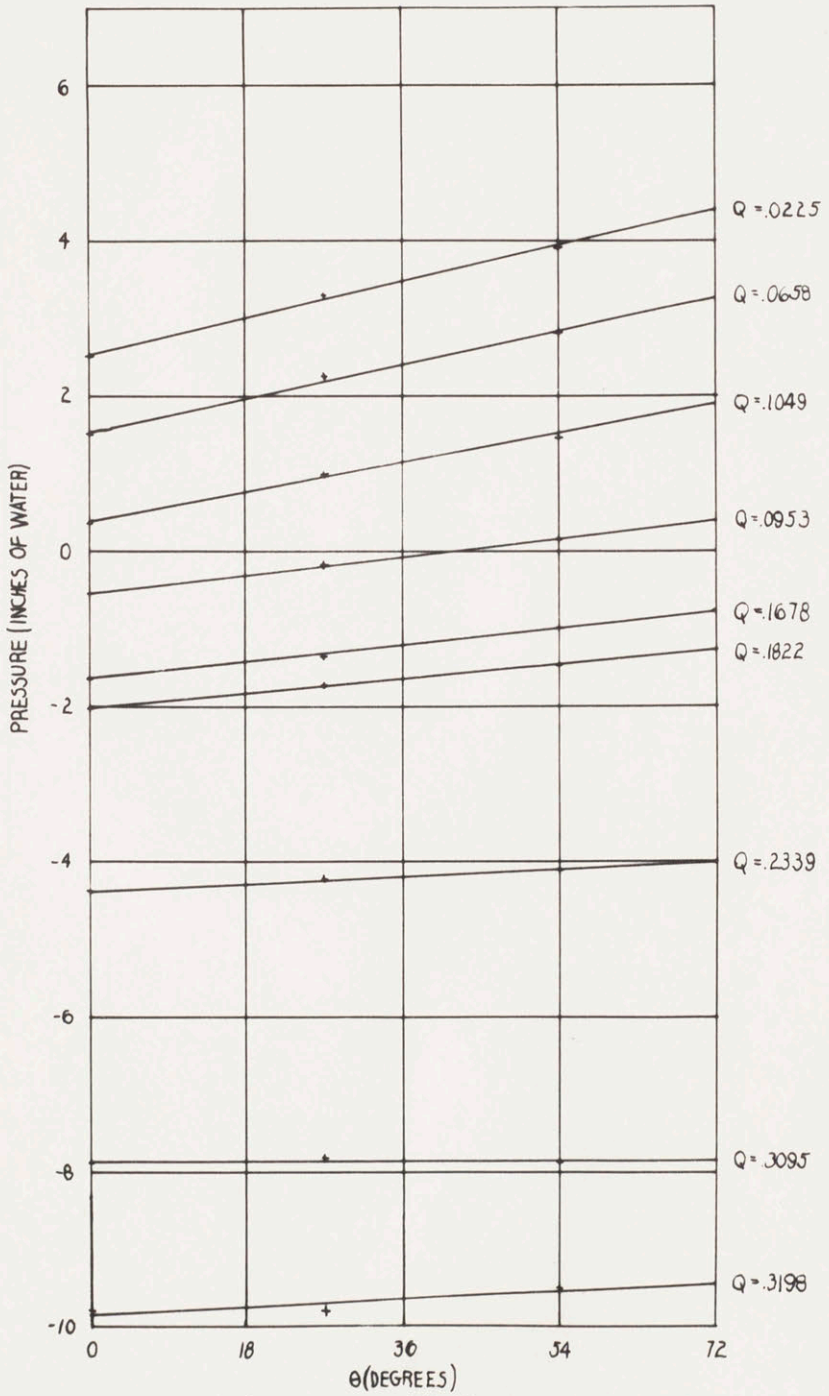

GRAPH OF PRESSURE VERSUS ANGLE AT A RADIUS OF 1.812" FOR DIFFERENT THROUGH-FLOWS (Q)(FT³/SEC OF AIR)

FIG. 26

SHROUDED IMPELLER

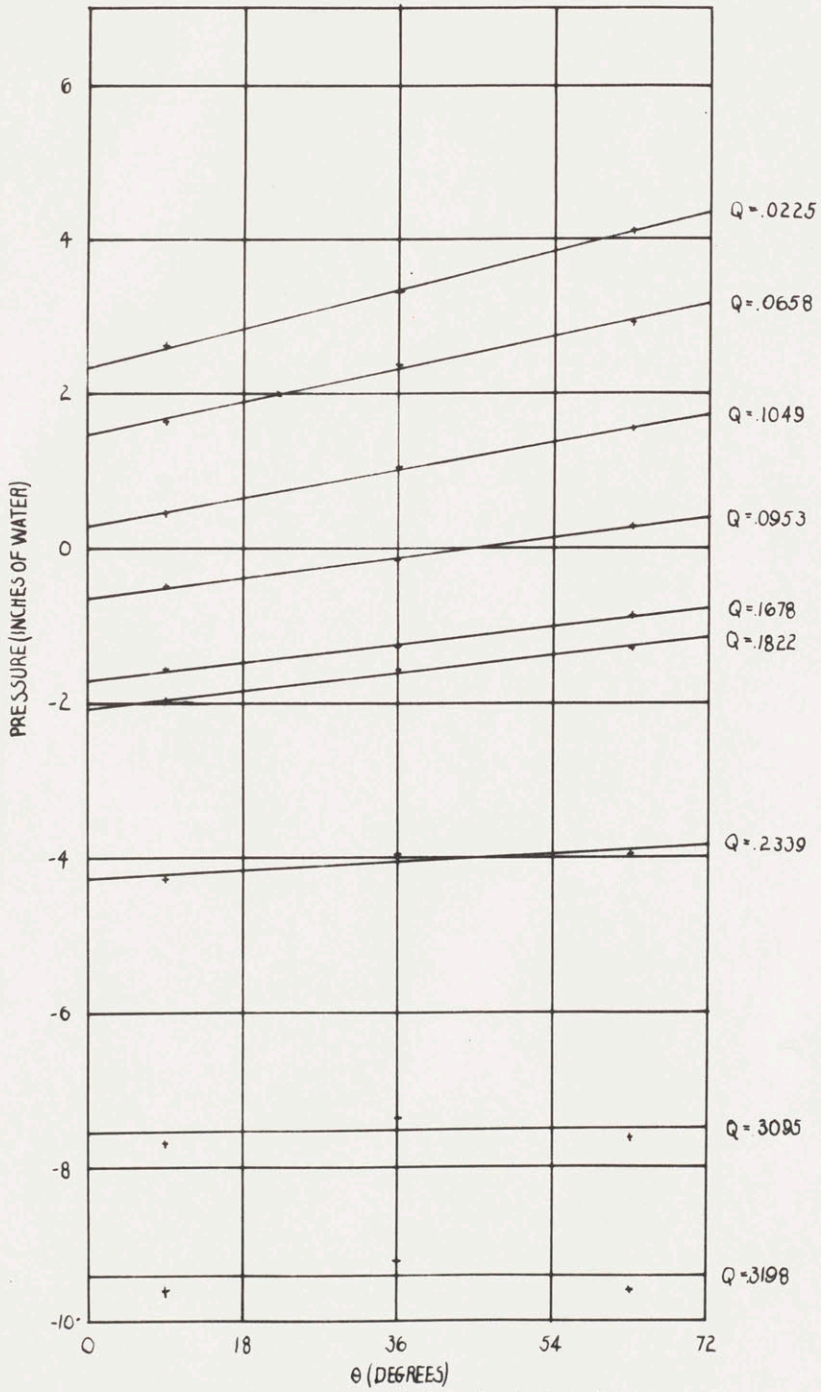

GRAPH OF PRESSURE VERSUS ANGLE AT A RADIUS OF 2.1" FOR DIFFERENT THROUGH-FLOWS (Q)(FT³/SEC OF AIR)

FIG. 27

SHROUDED IMPELLER

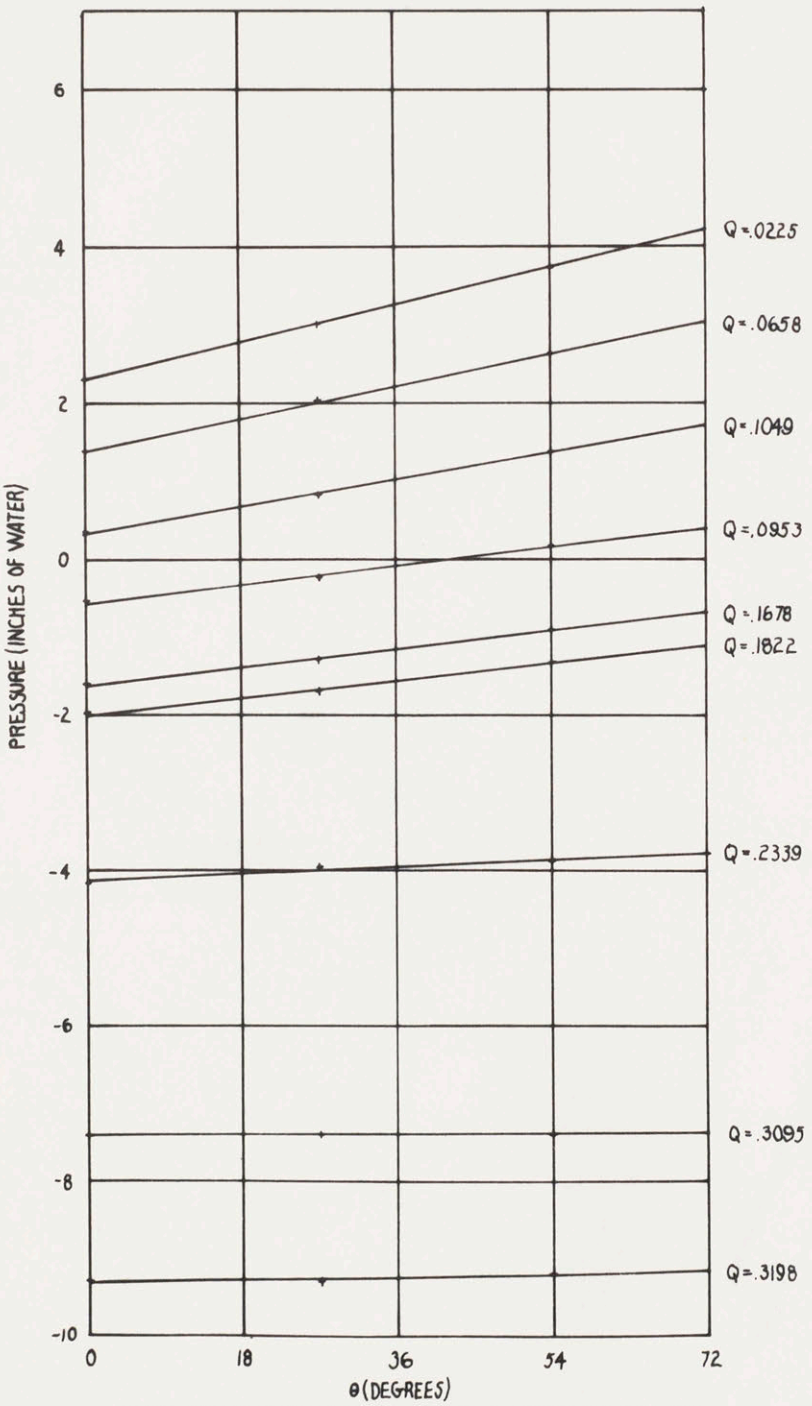

GRAPH OF PRESSURE VERSUS ANGLE AT A RADIUS OF 2.4" FOR DIFFERENT THROUGH-FLOWS (Q)(FT³/SEC OF AIR)

FIG. 28

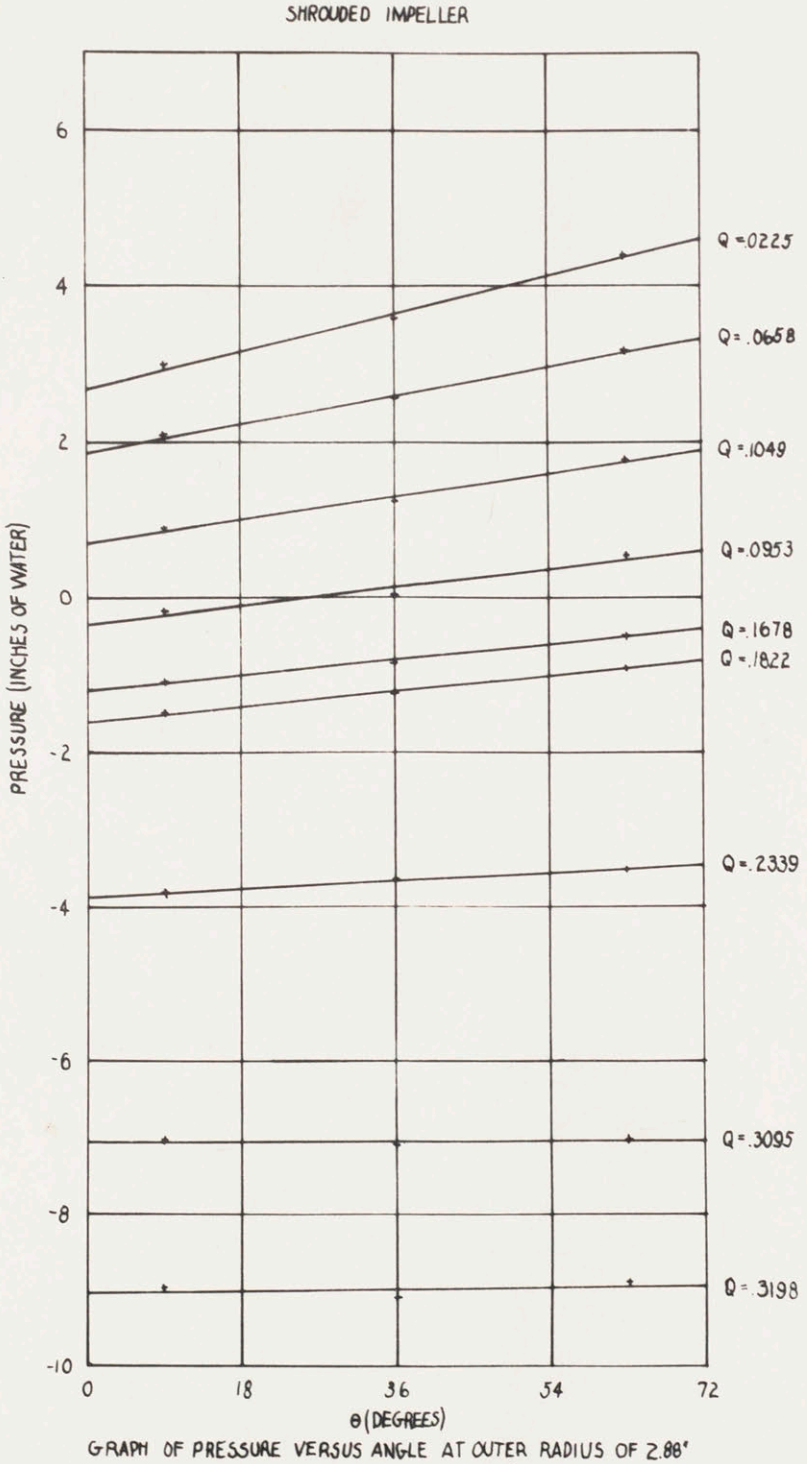

GRAPH OF PRESSURE VERSUS ANGLE AT OUTER RADIUS OF 2.88"
FOR DIFFERENT THROUGH-FLOWS (Q)(FT³/SEC OF AIR)

FIG. 29

SHROUDED IMPELLER

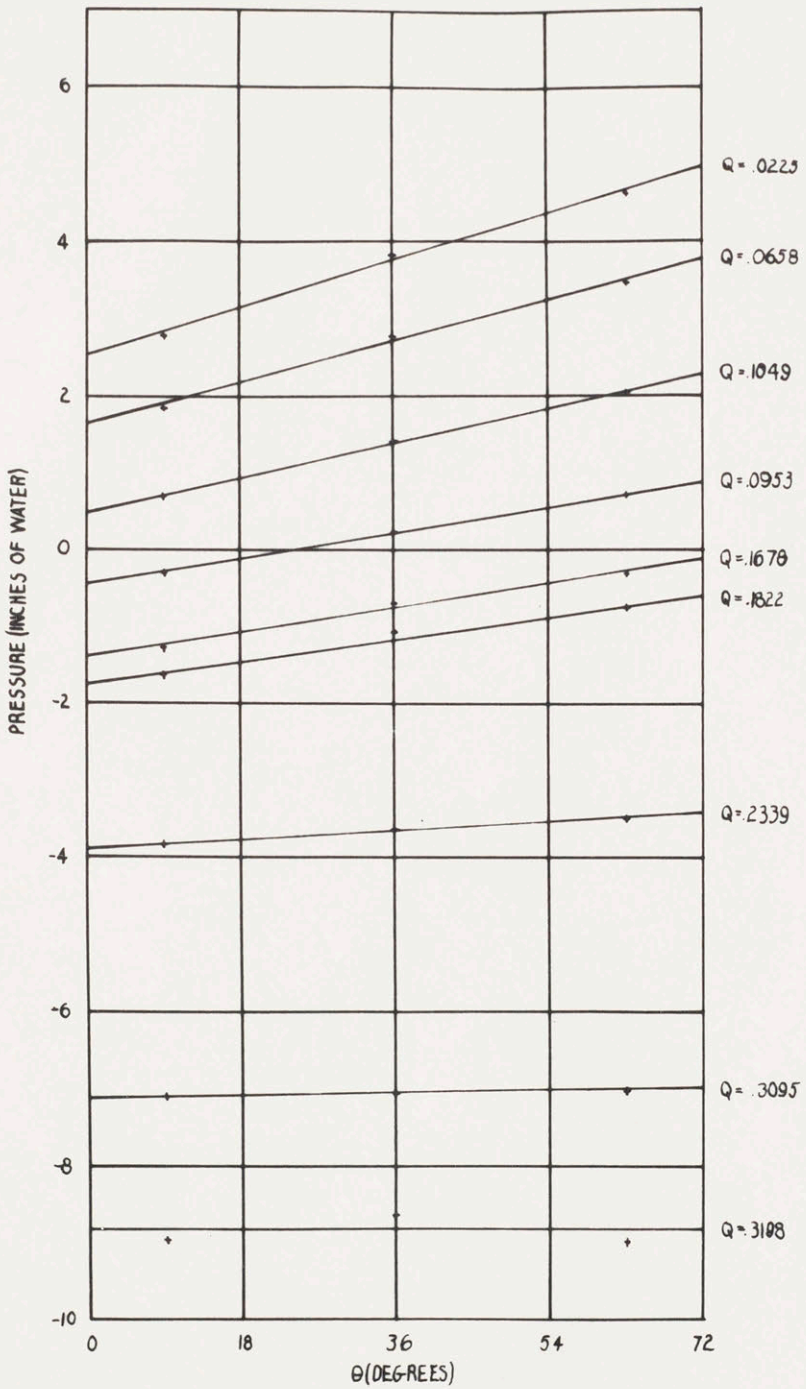

GRAPH OF PRESSURE VERSUS ANGLE AT INNER RADIUS OF 2.88"
FOR DIFFERENT THROUGH-FLOWS (Q)(FT³/SEC OF AIR)

SHROUDED IMPELLER

FIG. 30

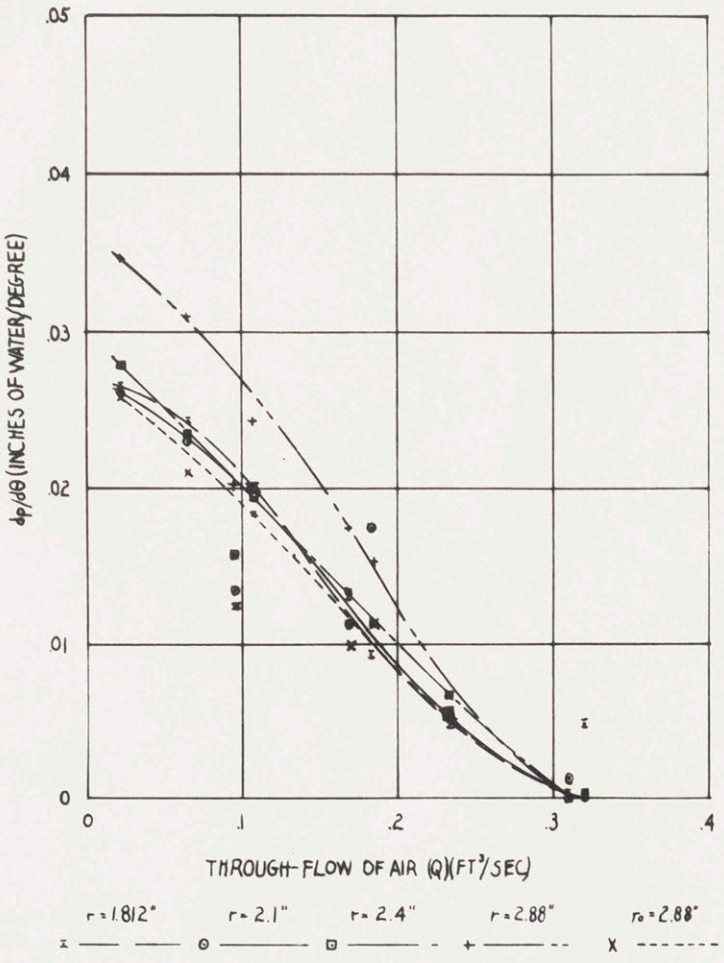

GRAPH OF dp/dθ VERSUS VERSUS THROUGH-FLOW

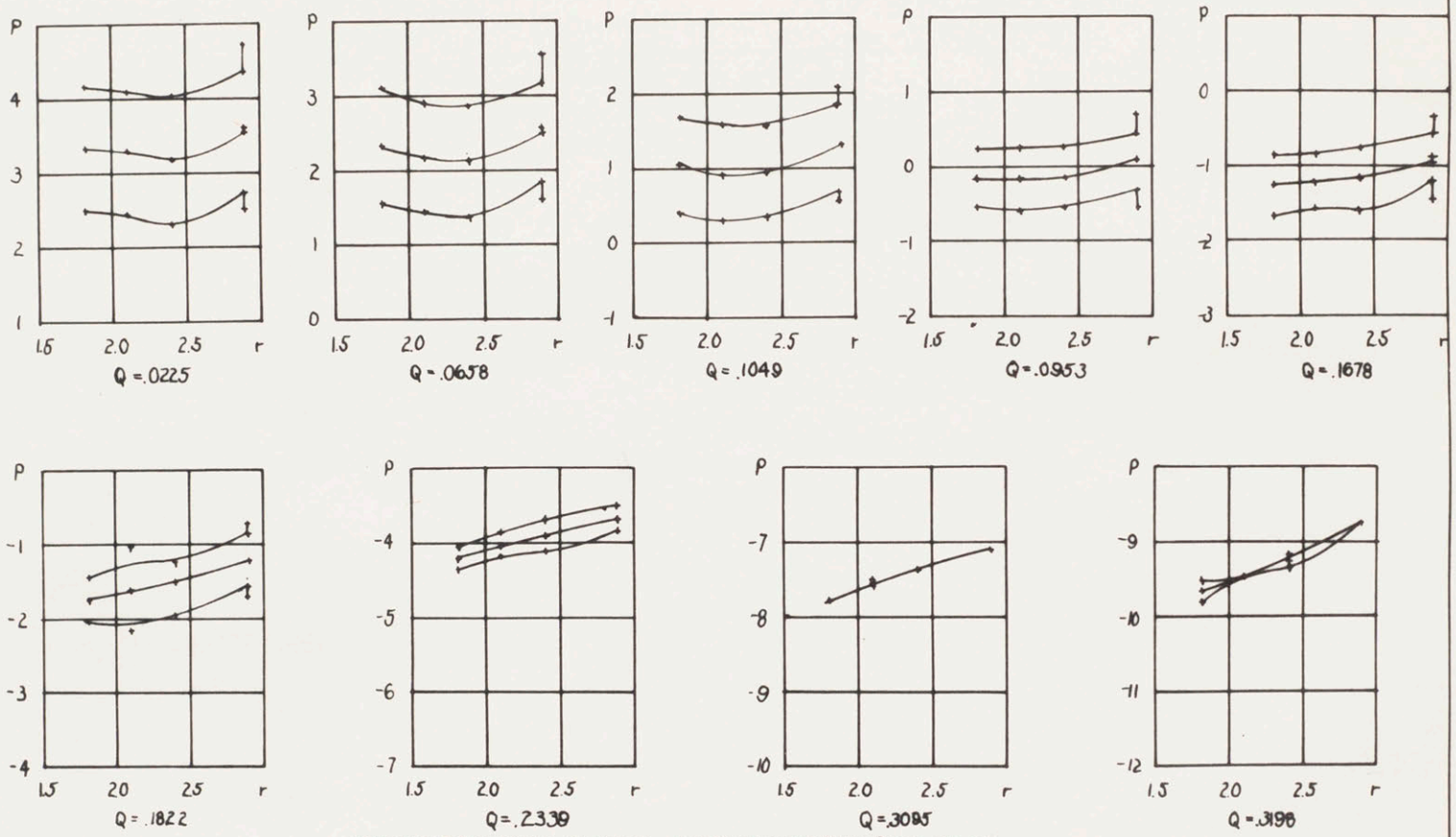

PRESSURE (P) IN INCHES OF WATER THROUGH-FLOW (Q) IN FT³/SEC OF AIR
RADIUS (r) IN INCHES

GRAPHS OF PRESSURE VERSUS RADIUS AT THREE ANGLES FOR DIFFERENT THROUGH-FLOWS
UPPER CURVES : $\theta = 63°$ MIDDLE CURVES : $\theta = 31.5°$ LOWER CURVES : $\theta = 0°$
SHROUDED IMPELLER

FIG. 31

Appendix on Calculations

Useful Horsepower: $\gamma Q(H_1-H_2)/550$

Where:

Q equals through flow in ft^3/sec

γ equals weight per unit volume in $lbs./ft^3$

(H_1-H_2) equals head rise across pump in ft. of air

Brake Horsepower = kwT

Where $k = 1/(12)(550)$ $ft\text{-}HP_{SEC}/ft\text{-}lb\text{-}in = 1.515x10$ HP-SEC in-lb

$w = 120\pi$ radians per second

T = torque in inch-pounds

$\gamma air = (14.65)(144)/(53.35)(536.8) = .0736\ lb/ft^3$

Through-flow = $Q = KAY\sqrt{2g\Delta P_{34}}$

Where

k = nozzle correction factor = .985

A = cross sectional area of channel = $.000667\ ft^2$ (not including bucket)

$Y^* = .52 + .48P_3/P_4 = 1 + .48(P_3-P_4)/P_4$, but P_3 measures vacuum. Therefore $Y = 1 - .48|(P_3-P_4)|/P_4$ where P is in ft of water.

$$Q = (.000667)(.985)(Y)\sqrt{\frac{(2)(32.2)(62.4)|(P_3-P_4)|}{.0736}}$$

$$.1532Y\sqrt{|(P_3-P_4)|}$$

---

* Flow correction factor derived from graph in Warner & Messersmith's "Mechanical Engineering Laboratory", pg.59

Calculations on solid body rotation

$dp/dr = \rho w^2 r$

Therefore $p = \rho w^2 r^2/2$ plus a constant

At radius 1.812", $p = \frac{(120)(1.812)(.074)}{(2)(32.2)(144)} = 3.73$ lbs/ft^2

At radius 2.88", $P = \frac{(120)(2.88)(.074)}{(2)(32.2)(144)} = 9.39$ lbs/ft^2

One inch of water gives a pressure of $\frac{62.3}{12} = 5.19$ lbs/ft^2

$\frac{P_{29}-P_{18}}{(5.19)} = \frac{9.39-3.73}{5.19} = 1.09$ inches of water

Miscellaneous Data

For Figures 1-4A, 12-19, 21-31

Temperature: 76.8 degrees Fahrenheit

Corrected atmospheric pressure: 29.913" Hg

For Figure 20

Temperature: 88 degrees Fahrenheit

Corrected atmospheric pressure: 29. 568" Hg

For Figure 5-11

Temperature: 78 degrees Fahrenheit

Corrected atmospheric pressure: 29.602" Hg

Descriptive Appendix

Contents

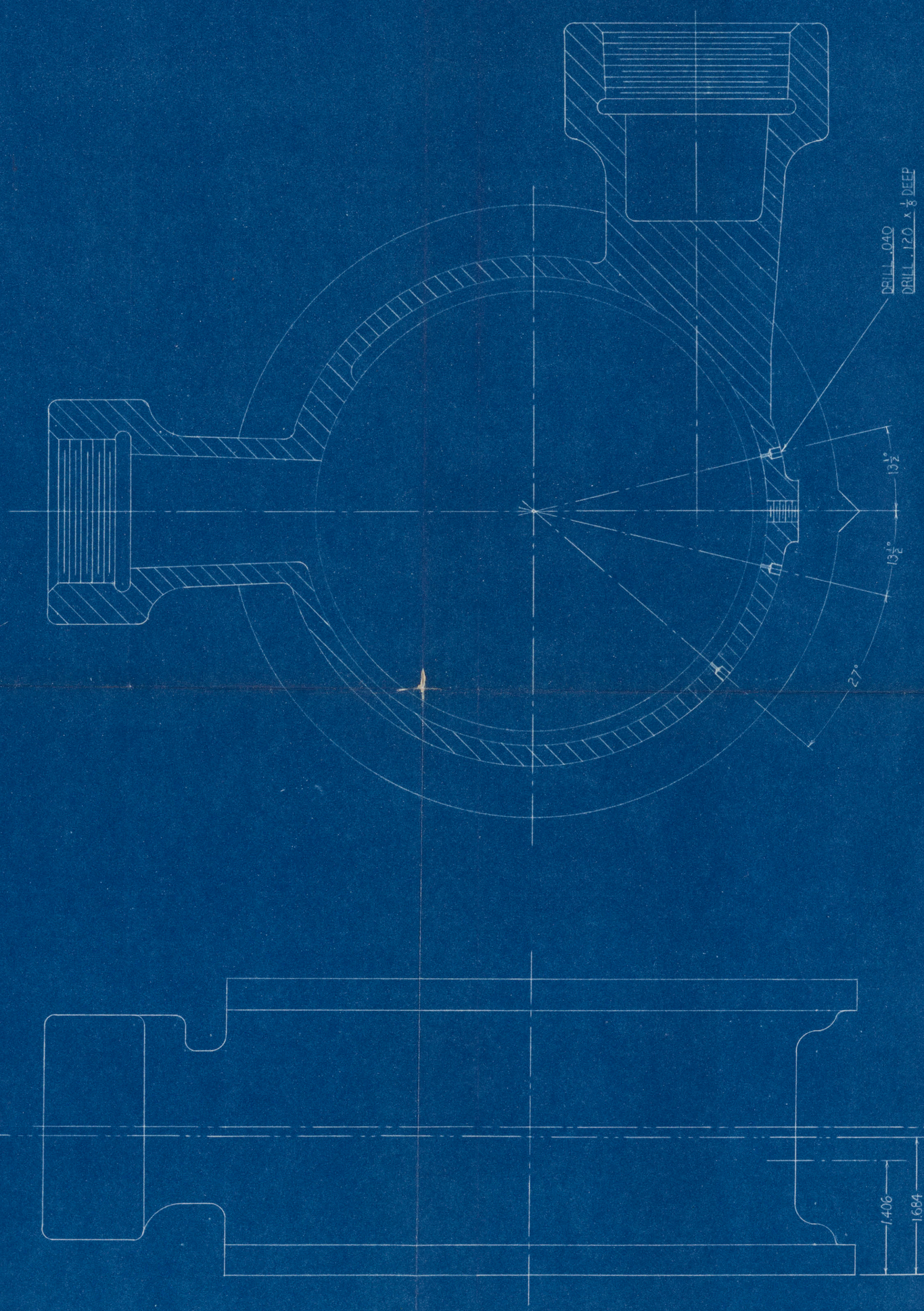

TOLERANCES:
DECIMAL ± .010
FRACTIONAL ± 1/64
ANGULAR ± ½°

M.E. DEPT. M.I.T.		STA-RITE REGENERATIVE PUMP	TH-7
CAST IRON	MAKE 1		
G. F. LUTZ	SCALE: FULL SIZE	CASE	2
	MAY 26, 1953		

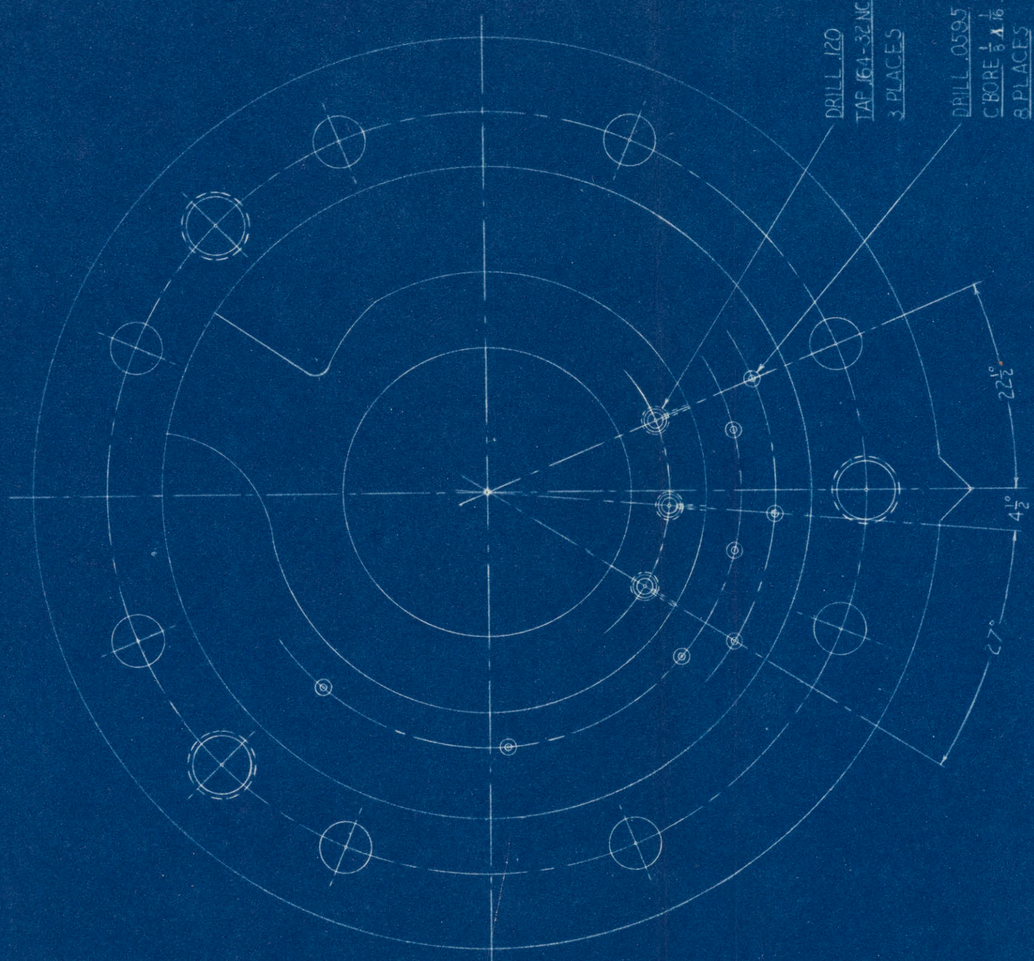

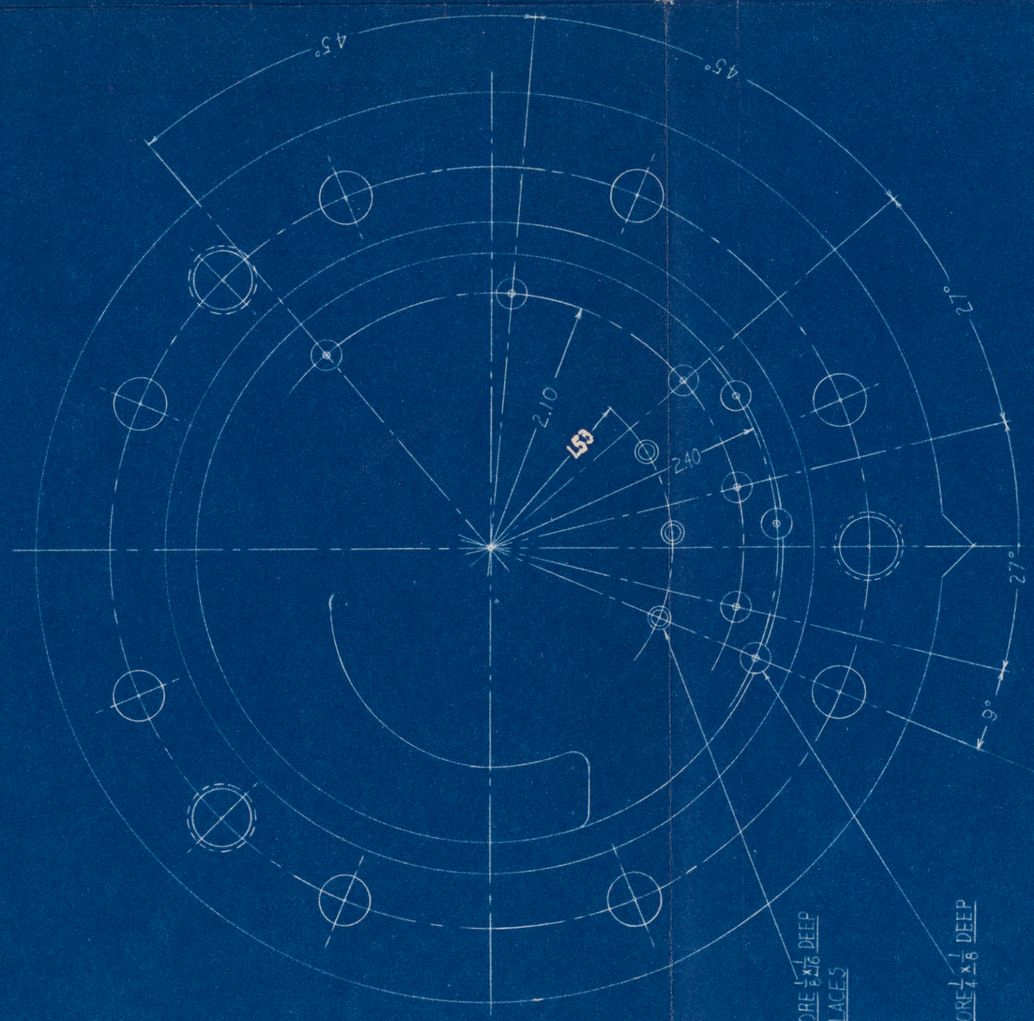

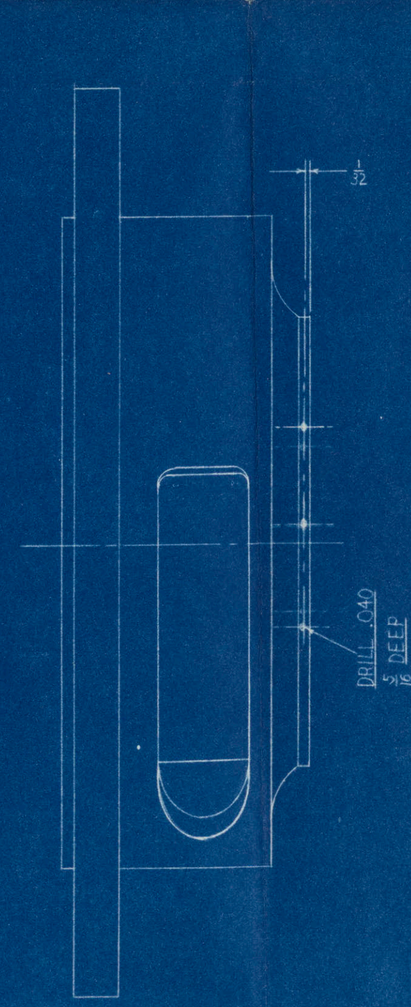

TOLERANCES:
DECIMAL ± .010
FRACTIONAL ± 1/64
ANGULAR ± 1/2°

M. E. DEPT. M.I.T.		STA-RITE REGENERATIVE PUMP	TH-7
CAST IRON	MAKE 1		
G. F. LUTZ	SCALE: FULL SIZE	MODIFIED FRONT HEAD	1
	MAY 25, 1953		

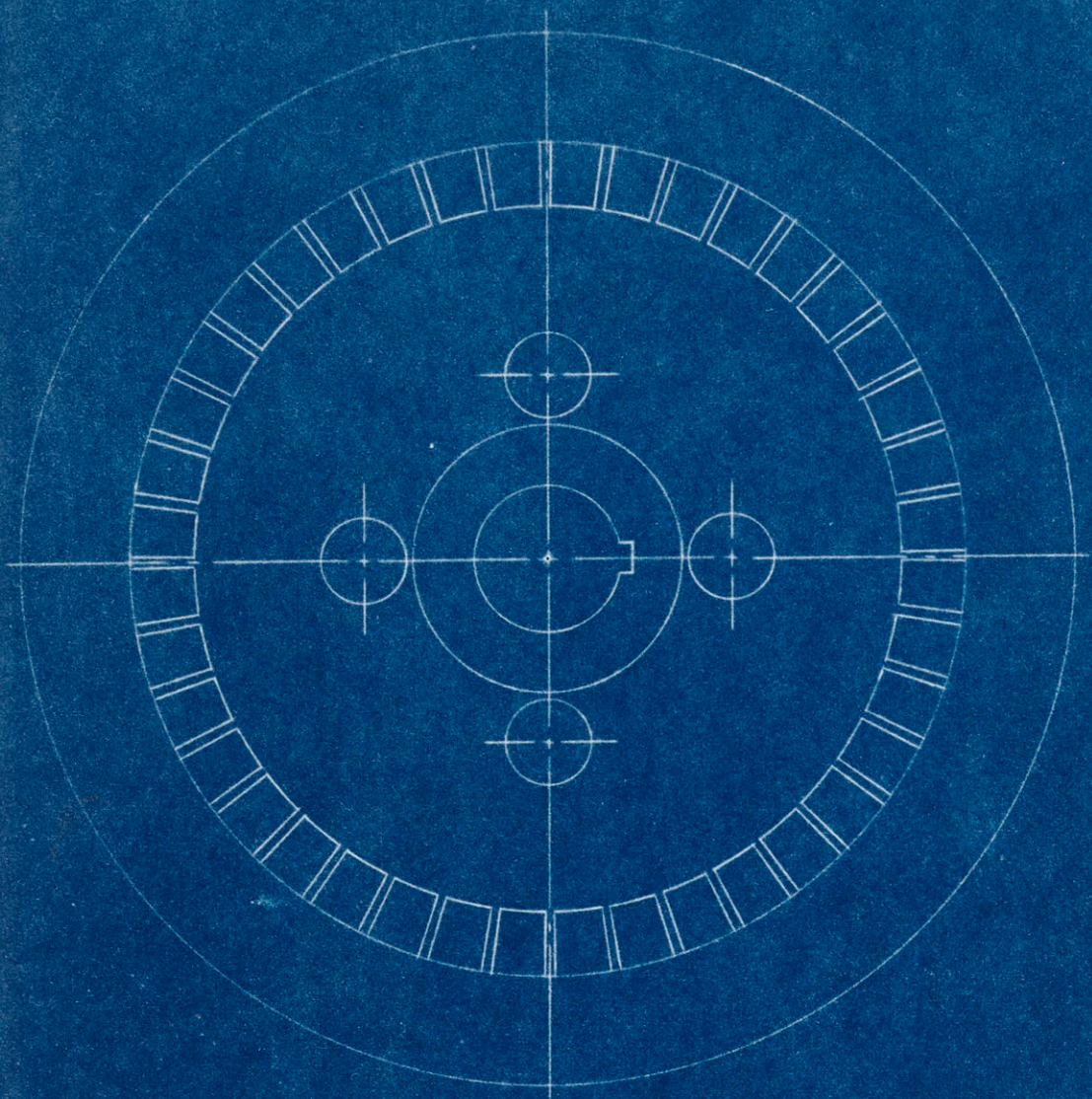

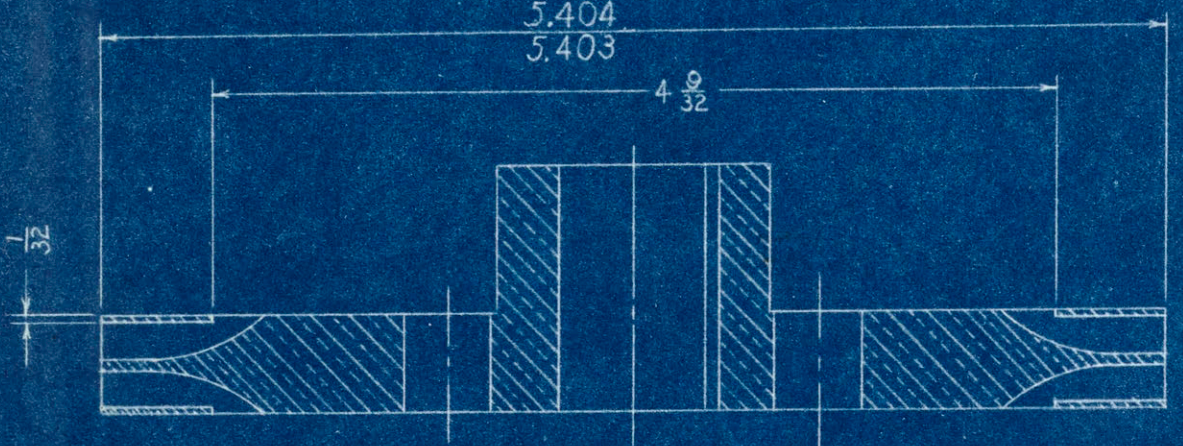

FRACTIONAL TOLERANCE ± 1/64

M.E. DEPT. M.I.T.		STA-RITE REGENERATIVE PUMP	TH-7
BRONZE ASTM 2A (NAVY M)	MAKE 1		
G. F. LUTZ	SCALE: FULL	SHROUDED IMPELLER	3
OLDER BRASS SHROUD TO IMPELLER	MAY 26, 1953		

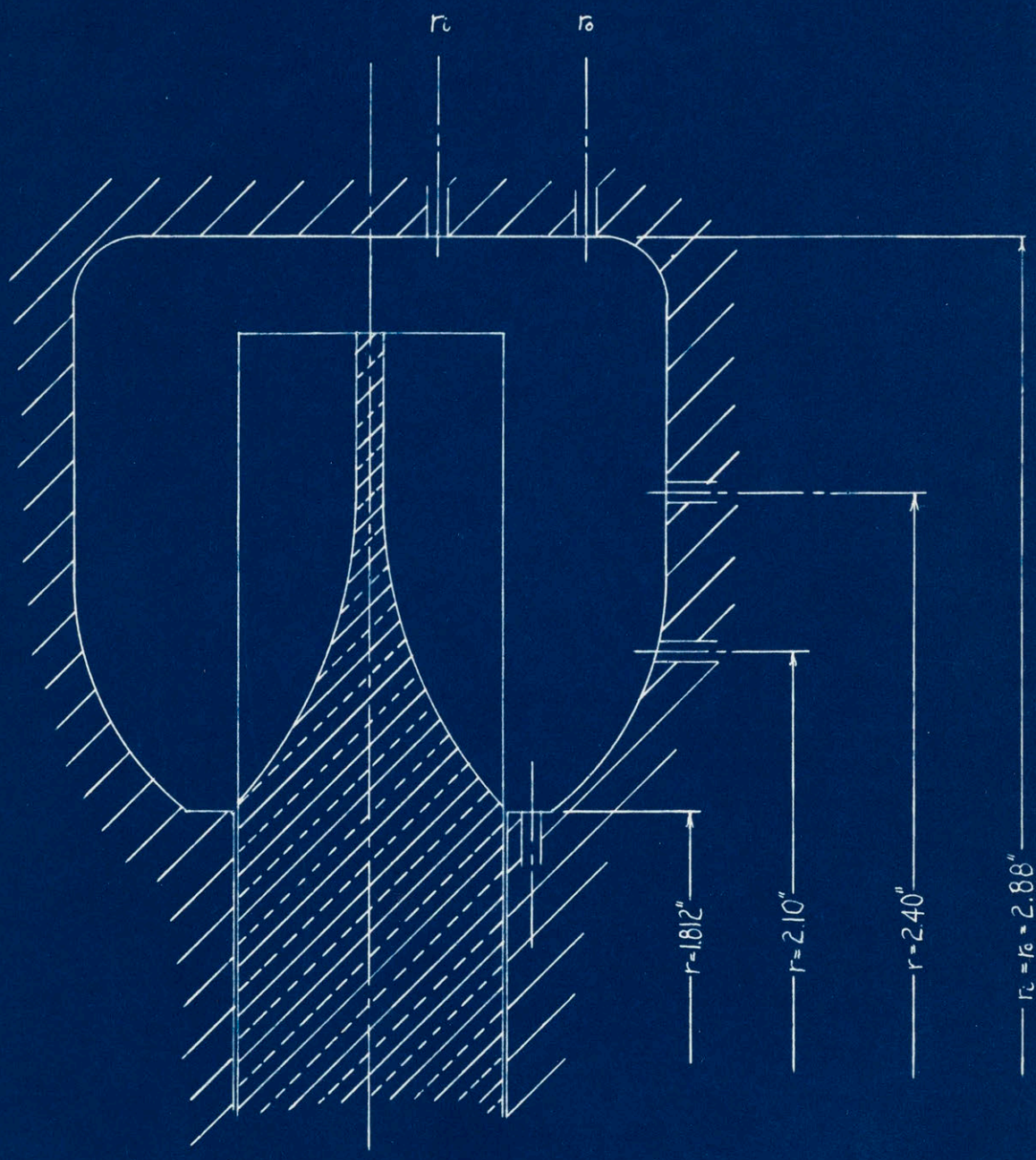

M.E. DEPT. M.I.T.		STA-RITE REGENERATIVE PUMP	TH-7
CAST IRON AND BRONZE			
G. F. LUTZ	SCALE: THRICE SIZE	PRESSURE TAP DETAIL	4
	MAY 26, 1953		

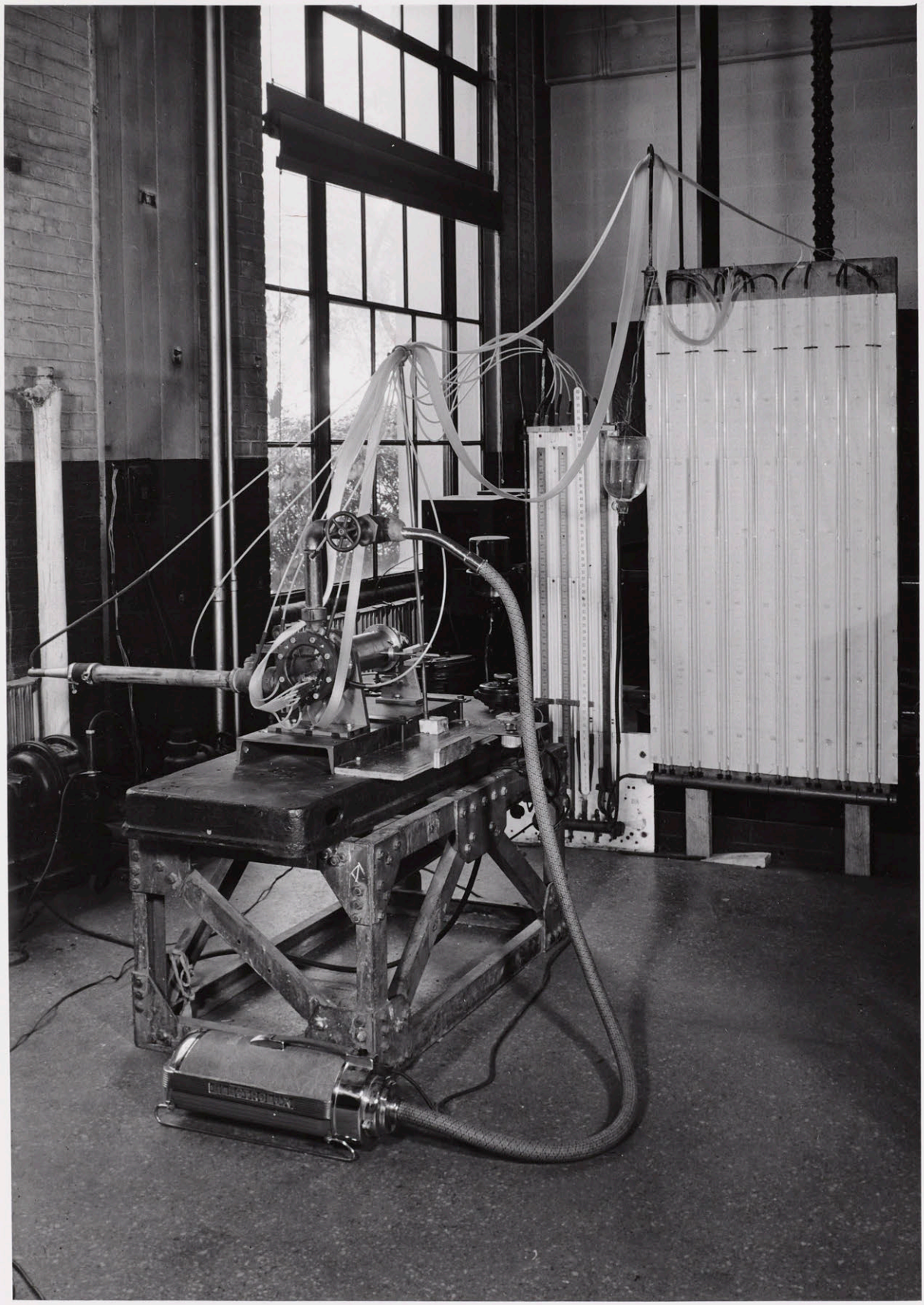

Plate I

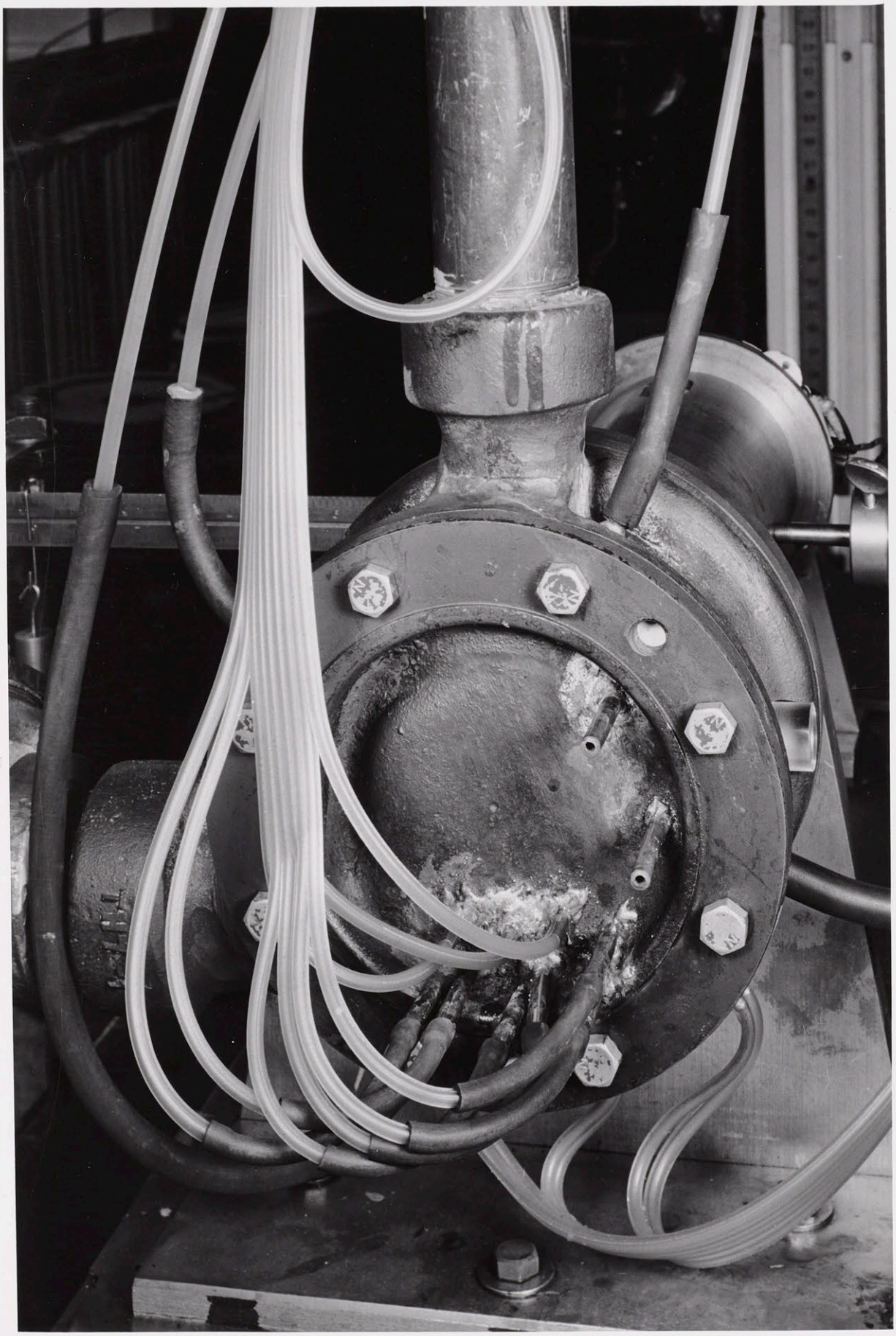

Plate 2

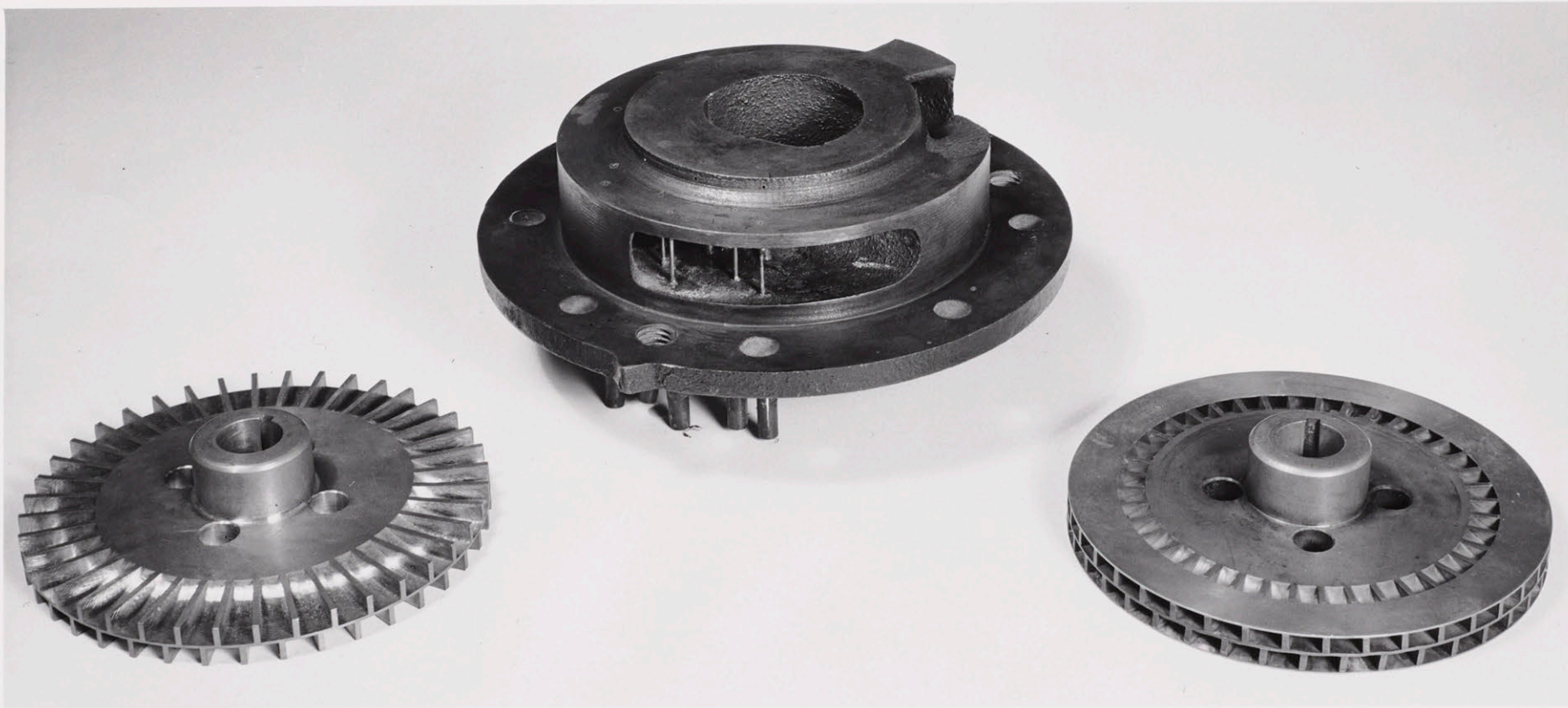

Plate 3

Bibliography

Lippman, D. and Taylor,T., "Design and Construction of Test Equipment for a Regenerative Fluid Pump"

Hopkins, T.and Lazo, L., "Theoretical and Experimental Analysis of a Regenerative Turbine Pump, the Sta-Rite TH-7"

Wislicenus, G.F., "Fluid Mechanics of Turbomachinery", McGraw-Hill, New York, 1947

Hunsaker and Rightmire, "Engineering Applications of Fluid Mechanics", McGraw-Hill, New York, 1947

Dean, R.C.Jr., "Aerodynamic Measurements", MIT Gas Turbine Laboratory, Cambridge, 1952

Warner & Messersmith 's "Mechanical Engineering Laboratory", John Wiley & Sons, New York, 1950